We thank the two reviewers for their useful and thoughtful comments and have incorporated their suggestions into the revised manuscript. Changes include adopting a different tropopause definition based on the vertical ozone gradient, adding surface temperature as a regression function, and quantifying the goodness-of-fit of the regression model using the coefficient of determination. Figures 2, 3, and 4, and Tables 2 and 3 have been modified as the consequence of such changes. We detail our responses and changes as below. The referees' comments are copied below, with our responses in bold. In our revised manuscript, the modified text is shown in bold, and the modified tables and figures are highlighted.

Anonymous Referee #1

This paper presents an interesting analysis of ozone variability above the observation site of Lauder in New Zealand. The objective is to identify and quantify the main drivers of ozone variability and trend at different altitudes as monitored with ozone sondes. The attribution is carried out using multivariate regression analysis and sensitivity simulations from a chemistry-climate model. A large part of the ozone variability is found to be driven by dynamical/climate variability. Some of it is also linked to changes in O3 precursors emissions. The results suggest that ozone long-term monitoring at specific sites contains valuable information in terms of the causes of ozone changes. This study illustrates how to extract information about atmospheric composition changes from ob-servational time series. The results will be useful to scientists running monitoring sites. The paper is reasonably clear and well written. Its scope fits perfectly with those of ACP. Therefore, I recommend publication with minor corrections that the authors may consider.

Thanks very much for the reviewer's positive comments.

l19, p2 : 'where climate change accelerates the export of O3 to higher latitudes, reducing O3' I think the impact of climate change on tropical ozone in the stratosphere is more about enhanced tropical uplift and hence reduced time for ozone production in rising air.

bf We have revised this sentence to "...but there may be no sustained recovery in the tropical lower stratosphere where climate change increases tropical upwelling, leading to less time for O3 production and hence reducing O3 in this region (Eyring et al., 2010)." (Page 2, lines 18-20)

l5, p3: for more clarity, I would suggest to have: 2.1 ozone record 2.2 statistical method 2.3 chemistry-climate model simulations

Thanks for the suggestion. We have now added subsections in Section 2.

l21, p3: 'Tropopause height is calculated using the 150 ppbv O3 chemical tropopause'. Why 150 pbbv ? Prather et al., 2011, recommended the 100 ppbv O3 contour. Prather, M. J., et al. (2011), An atmospheric chemist in search of the tropopause, J. Geophys. Res., 116, D04306, doi:10.1029/2010JD014939.

We have now adopted the definition of the tropopause based on vertical gradient of ozone, which is greater than 60 ppbv/km and remains so for a further 200 meters, constrained by ozone mixing ratio greater than 80 ppbv and exceeds 110 ppbv immediate above the tropopause (Bethan et al., 1996). This ozone tropopause definition has the advantage of being consistent with the PV definition (Beekmann et al., 1994, Bethan et al., 1996)). Consequently, we have recalculated the regression function and the trend of the observed and simulated tropopause height based on revised tropopause height, and revised figures (2, 3, and 4), tables (2 and 3), and the relevant text accordingly. Resultant changes are small. (Page 3, line 24-28)

l24, p3: The different model simulations are forced by different scenarios in CH4 and other O3 precursors, greenhouse gases (GHGs), and ozone depleting substances (ODSs) over the period of the time series. There does not seem to be any forcing that is characteristic of the effect of tropospheric O3 precursors.

We do not include short-lived ozone precursors in the regression as this would be difficult to formulate in terms of a usable, univariate regression function. Moreover, CH4 is the most effective ozone precursor in the remote Southern Hemisphere background air, but it doesn't impact ozone variability due to its well-mixed nature.

l24, p3: The effect of surface temperature is discussed in the text and appears in Table 3 (correlation coefficient). It seems to be the dominant factor in O3 variability at the surface. Why wasn't it included in the regression?

We have now included surface temperature as a regression function, and made changes accordingly. As a result, we have revised Figures 2 and 3, and Tables 2 and 3 accordingly, and have added related discussions in Section 3.1. (Page 3, Eqn. (1) and Sec. 3.1)

l20, p3: What is Cly? 'effective equivalent chlorine loading (Cly)'. and 2 lines down : 'Cly is the total chlorine loading'.

Thank you. We have now clarified that "Cly is the total chlorine loading". (Page 3, line 23)

l27, p3 : 'We note that interdependencies and correlations, e.g., between stratospheric temperature, relative humidity at surface, and tropopause height as regression functions, cannot be excluded'. There is no need to speculate here. For example, the effective equivalent chlorine loading, a regression function, impacts O3 and stratospheric temperature, one of the regression function. Furthermore, correlations between regression functions can be calculated. It is a significant source of uncertainties and should be discussed.

We have removed this sentence and have added a discussion of the correlations between regression functions in Section 3.1. (Page 6, lines 32-34 and page 7, lines 1-2)

l24, p4: 'CH4 mixing ratios are prescribed at the surface, and the same CH4 scenario is used in both chemistry and radiation.' The wording is a bit confusing. Isn't the model-calculated CH4 fed into the radiation scheme, like O3?

Yes, model-calculated CH4 (i.e. prescribed at the surface but subjected to transport and chemical removal) feeds into the radiation scheme. We have revised the text to make this clearer. (Page 5, lines 2-3)

l32, p4: This paragraph would greatly gain in clarity and usefulness if the different simulations were described and contrasted instead of just referring to the Table 1.

We have now modified the texts to make the description of this second set of CCMI simulations clearer. (Page 5, lines 10-12, 16-18)

l10, p5: 'Fig. 2 shows the deseasonalised O3 anomalies at the eight layers from the surface to the lower stratosphere, and the respective regressed O3 anomalies'. Please, could you indicate when a figure is about observed or model-calculated variables? Also, is it monthly means for all the analysis (as indicated in one figure)? Give more information about the time resolution and data processing/filtering of the different analyses.

We have added more details in Section 3.1 to achieve greater clarity. (Page 5, line 24-30)

l11, p5: Can be quantitative about the amount of variability captured by the regression? just provide the values of the determination coefficient R2.

We now present R2 in the new Table 2. We have also added some related discussions in Section 3.1. (Page 5 line 30 to page 6 line 3)

l19, p5: "project onto" ? replace by "are mostly driven by"

Changed.

l26, p5: se comment above about Tsurf missing from the regression.

Surface temperature (Tsurf) has now been added in the regression model (Eqn. (1)), and the text has been modified accordingly (Section 3.1).

l29, p6: it's very unlikely that temperature is the driver of O3 variability in the lower stratosphere. The slowing down of O3 destruction by stratospheric cooling (via Chapman cycle) occurs in the upper stratosphere. The ozone budget and variability in the mid-latitude lower stratosphere is dominating by dynamics. I think temperature changes simply reflect dynamical changes that drive O3 variability.

Agree. We have modified the text accordingly. Now it reads "In the stratosphere above 15 km, negative O_3 trends become weaker and are not significant at the 95% confidence level. Long-term changes in O_3 in this region are influenced by changes in dynamics (which are reflected in changes in stratospheric temperatures linked to O_3 changes), and O_3 depletion/recovery that is governed by changes in O_3 depleting substances; such changes seem to have cancelled out the decrease in O_3 resulting from the tropopause height increase in this region." (Page 7 lines 31-34 to page 8 line 1)

l9, p8: Difficult to expect a CCM to reproduce specific short-term O_3 anomalies. Those anomalies are often driven by specific dynamical variations. Comparisons between CCM simulations and observational time series make more sense when considering long term trends. I would suggest to add the analysis of a REF-C1SD simulation (wind/temperature forced by meteorological analyses instead of being calculated by the model) and compare to REF-C1. It would give an estimate about the effect of model-calculated dynamics/meteorology and biases (yes, there are some) on O_3 variability, including trend, for the considered site. Even on long-time series, this could be significant. The authors would be in a stronger position in their attribution analysis. It is less of a problem when considering large-scale averages or multiple sites but here the analysis is limited to a specific site.

We agree with the reviewer that a free-running CCM has limitations w.r.t. reproducing short-term O_3 anomalies. Unfortunately, we have not performed specified dynamics (SD) simulations for comparison with our RED-C1 simulation presented here. However, we did assess simulations by other CCMI models (REF-C1 and REF-C1SD) w.r.t. how their ozone compares to the Lauder ozone record. These other REF-C1 simulations often compare worse to the record than our own simulation. The REF-C1SD simulations usually better reproduce the O_3 variability in the stratosphere than REF-C1, but with mixed performance in the troposphere.

Therefore, for brevity and clarity, we have decided not to include SD simulations from different models here. The focus of this paper is on attribution of anthropogenic forcings to O3 trends at Lauder, and we believe that this is best achieved by contrasting sensitivity simulations to the reference simulation in a consistent model setup. Moreover, SD simulations are not suitable for use in the attribution study, due to externally imposed meteorological forcing, and in some cases are not self-consistent (r/f Hardiman et al. 2017). Free-running simulations have the merit being

more internally self-consistent, taking into account both dynamical and chemical feedbacks, and are more suitable for assessing long-term impact. We have now noted in the text that free-running CCMs have limitations in re-producing O3 variability and trends at one specific site. Furthermore, a comparison between free-running and SD simulations would be more meaningful in a multi-model and a multi-site context that will avoid any potentially biased conclusion, which is outside the scope of this study. We have added some discussions in the text. We hope this is satisfactory. (Page 9 lines 22-29)

We very much concur with the reviewer's point that it is important to compare free-running and SD simulations in reproducing O3 trends and variabilities in general, and we will pursue a following-up study to more comprehensively analyse multi-model results for more locations.

Figures : Can the authors add in all the figure captions which curves are what?

We have now added the description of each curve in respective figure captions.

Anonymous Referee #2

Review of Zeng et al. Attribution of recent ozone changes in the Southern Hemisphere mid-latitudes using statistical analysis and chemistry-climate model simulations

This study uses statistical analysis to understand recent changes in ozone up to 25 km at Lauder, NZ and relate them to changes over similar and longer time periods in chemistry-climate model simulations. Overall the manuscript is clearly written and analysis explained well and I think it would be of interest to the ACP community and would recommend its publication after the authors take some mostly minor comments into consideration.

Thanks very much for the reviewer's positive comments.

General comments:

I have concerns about using a chemical measure (O3) for tropopause height to evaluate the O3 field itself. Can you demonstrate that this measure is the same as a PV or temperature based tropopause height over varying timescales?

We agree that PV would be the ideal quantity to define the tropopause. Unfortunately, we don't have observed variables to calculate PV. We have modified our tropopause height definition to that of Bethan et al. (1996), based on the vertical ozone gradient, which is consistent with the PV definition (e.g., Beekmann et al. 1994). We have recalculated the tropopause height and have incorporated the new tropopause height in our regression analysis. Consequently, the trend in tropopause height at Lauder has changed from 14.2 m/yr to 17.9 m/yr. We have also calculated the tropopause height based on the WMO lapse rate definition, and the result is similar to that based on the ozone definition (trend: 16.5 m/yr). There is no significant systematic difference between the calculated ozone tropopause height and the thermal tropopause height at Lauder. We have revised the relevant text (page 3, lines 24-28), figures (2, 3, and 4) and tables (2 and 3) based on the new tropopause definition.

I can understand on shorter timescales how the level of o3 of 150 ppb would reflect dynamical variability in tropopause height (although one could argue that a different concentration - 100 ppb might be a better choice) but on longer timescales it seems like the chemical changes (through ODS changes) would also be reflected in this quantity. Can you quantify and separate and include some discussion in the text of this issue?

We have now adopted the new definition of tropopause height based on ozone gradient greater than 60 ppbv/km, constrained to ozone mixing ratios greater than 80 ppbv and exceeding 110 ppbv immediately above the tropopause (Bethan et al., 1996). Longer time-scale O3 changes will inevitably affect the tropopause movement through their feedbacks to the dynamics, and it is not straightforward to separate the influence from chemical changes and those from dynamical changes. We are confident that the new ozone tropopause definition adopted here is a robust choice, and is also consistent with the thermal tropopause height in this case. Moreover, O3 changes in the tropopause region over this period (1987-2014) at Lauder are around 17-25 ppbv, which is significantly smaller than the vertical O3 gradient in this region (typically 50-70 ppbv/km).

What does chemical O3 tropopause changes look like over the full ref-C2 run can you see the impact of ODS changes causing o3 loss and recovery reflected in this quantity? If you can't see this impact it would be a good demonstration that it is essentially a dynamics only representation over both short and long time-scales. If you do it can be quantified and related to the smaller change in ODSs over the Lauder record

Using the revised ozone tropopause definition, the calculated trend in tropopause height from the REF-C2 simulation averages about 1.2 m/yr over 1960-2090, and does show some difference between the ozone depletion (4.1 m/yr in 1960-2000) and recovery periods (0.9 m/yr in 2000-2090). Ozone changes do affect dynamics through feedbacks, so we see a larger than average change in tropopause height during the ozone depletion period. This is just for clarification; we do not intend to discuss this in great detail in the present paper.

I understand that the Lauder record 1987-2014 includes only a modest change in ODSs peaking in the 1990s with little net change so a linear trend might be expected to be flat but it doesn't rule out a some ozone loss in the early period and gain in the later period.

Both REF-C1 and REF-C2 show some loss of stratospheric O3 from 1990-2000 and recovery from 2000 onwards (Figures 9 and 10). So there is some O3 loss in the early period of the record and gain in the later period. But it is hard to ascertain such a signal from the O3 sonde record at Lauder, due to large variability in observed stratospheric O3. Notes have been added in the text (Page 12, lines 5-10)

Can you explain why the variables in Table 3 are in some cases different than those shown in Figure 3 like surface Temperature which seems to be highly correlated to lower troposphere ozone is not shown in figure 3.

We have added surface temperature as a regression function and related discussions, and have modified Tables 2 and 3, and Figures 2 and 3. (Sections 2.2 and 3.1)

p5 line 17-18 it seems a bit circular argument if you are using o3 to define the tropopause height.

We have changed the definition of tropopause to be based on the vertical ozone gradient, and the statement stands.

p10 line1-3 Can you make the same claim for ODS changes over this time refC1 time period (difference between RefC1 and fODS).

We did not perform a "SEN-C1-fODS" scenario which could be compared to the REF-C1 simulation, therefore cannot directly compare between them. The SEN-C2-fODS simulation cannot be directly compared to the REF-C1 simulation due to differences in model constellation between them.

p10 line 34 p11 line 1-2 it is not obvious why this should be the case, can you do any additional analysis to explain possible mechanisms.

Unfortunately, we cannot explain the response of stratospheric O3 trend changes to changes in O3 precursors, which are mainly originated from the troposphere, based on current diagnostics and model simulations. We suspect it is caused by dynamical changes through chemical feedbacks to radiation. We plan to follow up with a more objective analysis. We have added a note to this effect in the text. (Section 4.4; Page 12 lines 14-16)

Attribution of recent ozone changes in the Southern Hemisphere mid-latitudes using statistical analysis and chemistry-climate model simulations

Guang Zeng[1], Olaf Morgenstern[1], Hisako Shiona[2], Alan J. Thomas[3], Richard R. Querel[3], and Sylvia E. Nichol[1]

[1]National Institute of Water and Atmospheric Research, Wellington, New Zealand
[2]National Institute of Water and Atmospheric Research, Christchurch, New Zealand
[3]National Institute of Water and Atmospheric Research, Lauder, New Zealand

Correspondence to: Guang Zeng (guang.zeng@niwa.co.nz)

Abstract.

Ozone (O_3) trends and variability from a 28-year (1987-2014) ozonesonde record at Lauder, New Zealand, have been analysed and interpreted using a statistical model and a global chemistry-climate model (CCM). Lauder is a clean rural measurement site often representative of the Southern Hemisphere (SH) mid-latitude background atmosphere. O_3 trends over this period at this location are characterised by a significant positive trend below 6 km, a significant negative trend in the tropopause region and the lower stratosphere between 9 to 15 km, and no significant trend in the free troposphere (6-9 km) and the stratosphere above 15 km. We find that significant positive trends in lower tropospheric ozone are correlated with increasing temperature and decreasing relative humidity at the surface over this period, whereas significant negative trends in the upper troposphere and the lower stratosphere appear to be strongly linked to an upward trend of the tropopause height. Relative humidity and the tropopause height also dominate O_3 variability at Lauder in the lower troposphere and the tropopause region, respectively. We perform an attribution of these trends to anthropogenic forcings including O_3 precursors, greenhouse gases (GHGs), and O_3 depleting substances (ODSs), using CCM simulations. Results indicate that changes in anthropogenic O_3 precursors contribute significantly to stratospheric O_3 reduction, changes in ODSs contribute significantly to tropospheric O_3 reduction, and increased GHGs contribute significantly to stratospheric O_3 increases at Lauder. Methane (CH_4) likely contributes positively to O_3 trends in both the troposphere and the stratosphere, but the contribution is not significant at the 95% confidence level over this period. An extended analysis of CCM results covering 1960-2010 (i.e. starting well before the observations) reveals significant contributions from all forcings to O_3 trends at Lauder, i.e., increases of GHGs and the increase of CH_4 alone all contribute significantly to O_3 increases, net increases of ODSs lead to O_3 reduction, and increases of non-methane O_3 precursors cause O_3 increases in the troposphere and reductions in the stratosphere. This study suggests that a long-term ozonesonde record obtained at a SH mid-latitude background site (corroborated by a surface O_3 record at a nearby SH mid-latitude site, Baring Head, which also shows a significant positive trend) is a useful indicator for detecting atmospheric composition and climate change associated with human activities.

1 Introduction

Ozone (O_3) is an important trace gas in the Earth's atmosphere, playing a central role in atmospheric chemistry and the radiation budget. Stratospheric O_3 prevents harmful UV light from reaching the Earth's surface and is also a source of tropospheric ozone via cross tropopause exchange. Tropospheric O_3 is formed by photochemical production in the presence of nitrogen oxides and volatile organic compounds (VOC). It controls the atmospheric oxidizing capacity through photolysis and subsequent reaction with water vapour to produce the hydroxyl radical (OH). Tropospheric O_3 is inhomogeneously distributed and highly dependent on the distributions of its precursors and on tranport. High levels of surface O_3 have adverse effects on human health and vegetation. Since the industrial era, surface O_3 in the Northern Hemisphere (NH) has increased substantially (e.g., Volz and Kley, 1988; Thompson, 1992) due to human activities. By contrast, surface O_3 in the Southern Hemisphere (SH) is more stable due to limited land and a general lack of precursor emissions. Here, surface O_3 is the result of stratosphere-troposphere exchange (STE) and methane (CH_4) oxidation.

In the SH, stratospheric O_3 changes, which are dominated by Antarctic ozone depletion, show significant negative trends especially at mid- to high-latitudes from the 1980s to the end of the 1990s (WMO, 2011). Reductions in stratospheric halogen due to the implementation of the Montreal Protocol would increase both tropospheric and stratospheric O_3; indeed, observations show that stratospheric O_3 between 35-45 km has shown no trend since the late 1990s (Figure 2-5 in WMO (2014)). However, ozone recovery is modulated by climate change. Model simulations show that recovery will occur between 2030 and 2070 (depending on region), but there may be no sustained recovery in the ~~tropics~~ **tropical lower stratosphere where climate change increases tropical upwelling, leading to less time for O_3 production and hence reducing O_3 in this region (Eyring et al., 2010)**. As a consequence, future changes of stratospheric O_3 will significantly impact tropospheric O_3 and potentially air quality (e.g., Zeng et al., 2010).

Understanding past O_3 changes and projecting the future O_3 evolution are of great importance to assessing future environmental changes. To cover its spatial and temporal variability, an extensive global ozone monitoring network exists measuring total column ozone, vertical profiles, and surface ozone. These measurements cover years to decades. Oltmans et al. (2013) analyse tropospheric O_3 trends from a large suite of surface O_3 and ozonesonde measurements for the past 20-40 years and find that there is no significant overall change in tropospheric O_3 in the NH and tropics; they attribute this no-growth to controls on O_3 precursor emissions after earlier increases of tropospheric O_3. However, in the SH subtropics and mid-latitudes, near-surface O_3 exhibits a significant positive trend since the 1980s but there have been no trends in the free and upper troposphere; reasons for this behaviour are not understood.

In this paper, we present the updated ozonesonde record covering 1987-2014 from Lauder, New Zealand (45ºS, 170ºE, 370 m above sea level), a clean rural site that is representative of the SH mid-latitude background atmosphere. Parts of the time series have been shown previously by Oltmans et al. (2006, 2013). Here, we focus on analysing and interpreting the tropospheric and lower stratospheric O_3 changes using a simple statistical model and global chemistry-climate model (CCM) simulations, and

identify the underlying dynamical and chemical changes that could contribute to the observed O_3 trends at this location, which also represent the evolution of background O_3 in the SH mid-latitudes in general. Although we mainly analyse the ozonesonde record at Lauder, the surface O_3 record at another SH mid-latitude site, Baring Head, New Zealand, will also be presented for comparison. We describe the ozonesonde time series, the statistical model used, and the chemistry-climate model simulations in the following section. Results are presented in Sect. 3, and conclusions are drawn in Sect. 4.

2 Ozone records, statistical method, and chemistry-climate model simulations

2.1 Ozone record

Weekly Electrochemical Cell (ECC) ozonesondes, launched at Lauder since August 1986, measure profiles of O_3, temperature, pressure and winds from the surface to about 35 km. The ozonesondes used are ECC EN-SCI IZ-series operating with a 0.5% buffered potassium iodide (KI) cathode solution (Boyd et al., 1998). Corrections are applied to the ozonesonde values above 200 hPa to account for pump efficiency degradation at low pressures (Bodeker et al., 1998). The integrated O_3 profile is compared to the total column of ozone measured by the Dobson spectrophotometer at Lauder; the relative difference is typically less than 5% (Bodeker et al., 1998). For this analysis, following Oltmans et al. (2013), we calculate vertically averaged O_3 mixing ratios for eight layers, namely, 0-1.5 km, 1.5-3 km, 3-6 km, 6-9 km, 9-12 km, 12-15 km, 15-20 km, and 20-25 km. Separate linear trends are then calculated for O_3 anomalies at each layer and over the whole period.

2.2 Statistical method

We construct a regression model to identify the dominant factors that are associated with O_3 variations and trends. The regression model includes bf nine time-varying forcings, i.e., the Solar Index (SI) which captures solar variability and is defined by the solar radio flux at F10.7 cm (data source: https://www.esrl.noaa.gov/psd/data/correlation/solar.data), the Multivariate El Niño Southern Oscillation Index (MEI) (https://www.esrl.noaa.gov/psd/enso/mei/), the Quasi-Biennial Oscillation at 30 hPa and 10 hPa, respectively (QBO_{30} and QBO_{10}) (http://www.esrl.noaa.gov/psd/data/climateindices/list/), relative humidity at the surface (RH_{surf}), **surface temperature (**T_{surf}**)**, stratospheric temperature averaged over 20-25 km (T_{strat}), tropopause height (HT_{Trop}), and the ~~effective equivalent~~ **total** chlorine loading (Cl_y). RH_{surf}, T_{surf} and T_{strat} are measured together with O_3 by the ozonesondes. **We define the tropopause as the minimum altitude where the vertical gradient of the ozone VMR is greater than 60 ppbv/km, remains so for a further 200 m, and the O_3 mixing ratio is greater than 80 ppbv, exceeding 110 ppbv immediately above the tropopause (ozone tropopause; Bethan et al. (1996)). The ozone tropopause definition is consistent with the definition of the dynamical tropopause based on potential vorticity (e.g., Beekmann et al., 1994).** ~~calculated using the 150 ppbv O_3 chemical tropopause, defined using observed O_3 at Lauder.~~ The total chlorine loading at 20 km over Lauder is taken from a transient CCM simulation assuming the WMO A1 scenario (WMO, 2011). The

regressed O_3 anomaly is expressed as

$$Ozone(t) = A * t + a_1 * SI(t) + a_2 * MEI(t) + a_3 * QBO_{10}(t) + a_4 * QBO_{30}(t)$$
$$+a_5 * RH_{surf}(t) + a_6 * T_{surf}(t) + a_7 * T_{strat}(t) + a_8 * HT_{Trop}(t) + a_9 * Cl_y(t), \quad (1)$$

of which $A * t$ is the linear component, and a_{1-9} are the regression coefficients for the corresponding regressors. All forcings are standardised but not de-trended. ~~We note that interdependencies and correlations, e.g., between stratospheric temperature, relative humidity at surface, and tropopause height as regression functions, cannot be excluded.~~ Observations as well as basis functions are monthly mean data.

2.3 Chemistry-climate model simulations

We perform and analyse a suite of sensitivity simulations with different model configurations aimed at investigating the factors that potentially contribute to observed O_3 trends at Lauder, e.g., CH_4 and other O_3 precursors, greenhouse gases (GHGs), and ozone depleting substances (ODSs) over the period of the time series (1987-2014). The model simulations we analyse here are from the National Institute of Water and Atmospheric Research-United Kingdom Chemistry and Aerosols (NIWA-UKCA) model, which comprises a detailed representation of stratospheric and tropospheric chemistry and is optionally run in atmosphere-only mode or coupled to a deep-ocean model. Detailed descriptions of the model are given by Morgenstern et al. (2009, 2017), O'Connor et al. (2014), and Zeng et al. (2015). We only give a brief description of the version used here. The background climate model is an early version of HadGEM3-A (Hewitt et al., 2011) at a horizontal resolution of $3.75° \times 2.5°$, with 60 levels from the surface to 84 km. Chemistry combines the stratospheric mechanism described by Morgenstern et al. (2009) and the tropospheric mechanism used by Zeng et al. (2008). Eight primary pollutants are emitted at the surface, namely nitrogen oxides (NO_x), carbon monoxide (CO), formaldehyde (CH_2O), ethane (C_2H_6), acetaldehyde (CH_3CHO), propane (C_3H_8), acetone (CH_3COCH_3), and isoprene (C_5H_8). We assume uniform, constant lower boundary conditions for nitrous oxide (N_2O), CH_4, hydrogen (H_2), and organic halogen compounds. Chlorine and bromine source gases are lumped, and we only explicitly model $CFCl_3$, CF_2Cl_2, CH_3Br, CH_2Br_2, and $CHBr_3$ here. Aerosol and aerosol precursor emissions are included. Lightning emissions of NO_x are parameterized as a function of cloud top height that is linked to convection in the model (Price and Rind, 1992, 1994). The model uses the FAST-JX interactive photolysis scheme (Neu et al., 2007; Telford et al., 2013) with a correction added above 60 km for photolysis occurring at wavelengths shorter than 177 nm (Lary and Pyle, 1991).

All simulations used in this study are listed in Table 1; they are part of the Chemistry Climate Model Initiative (CCMI) model simulations (Eyring et al., 2013; Morgenstern et al., 2017). The model data can be downloaded from the British Atmospheric Data Centre (BADC) (http://blogs.reading.ac.uk/ccmi/badc-data-access). We keep the experiment identifications as defined by Eyring et al. (2013) and Morgenstern et al. (2017) for CCMI. REF-C1 is a hindcast experiment using prescribed observed monthly mean sea surface temperatures (SSTs) and sea ice (HadISST; Rayner et al., 2003)) over the period of 1960-2010. Other forcings, e.g., GHGs, ODSs, and aerosol and aerosol precursor emissions follow state-of-knowledge historical evolutions from 1960 to 2010 (Morgenstern et al., 2017). The anthropogenic emissions of O_3 precursors are inter-annually varying following the MACCity scenario from 1960 to 2010 (Granier et al., 2011), and biogenic emissions are prescribed following the MEGAN2.1

(Guenther et al., 2012) dataset with no inter-annual variation. CH_4 mixing ratios are prescribed at the surface. ~~and the same CH_4 scenario is used in both chemistry and radiation~~. In this set up, chemistry is interactive, in that calculated O_3 and **CH_4 are** fed into the radiation scheme. We consider REF-C1 to be the state-of-knowledge experiment of the evolution of chemical composition from 1960 to 2010. We also performed a simulation with non-methane O_3 precursor emissions fixed at the 1960 level (SEN-C1-fEMIS) to assess the impact of increases in these emissions since 1960. Here we analyse the results between 1987 and 2010, to coincide with the Lauder ozonesonde measurements. In addition, we specify a stratospheric O_3 tracer (O_3S) to examine the impact of stratosphere-troposphere exchange (STE) on tropospheric O_3 in experiment REF-C1. O_3S is defined as having the same chemical destruction as the "normal" chemical O_3 tracer but no chemical production in the troposphere, to account for the O_3 that is originated from the stratosphere.

The second set of simulations are used to attribute O_3 changes to ODSs and GHGs, and are listed in Table 1. These simulations are carried out using the coupled atmosphere-ocean configuration. REF-C2 is the reference simulation covering the period of 1960-2100, and follow the WMO (2011) A1 scenario for ODSs and the Representative Concentration Pathway (RCP) 6.0 (Meinshausen et al., 2011) for other GHGs, tropospheric O_3 precursors, and aerosol and aerosol precursor emissions. For anthropogenic O_3 precursor emissions, we use MACCity emissions until 2000, followed by RCP 6.0 emission, as recommended for CCMI simulations. Unfortunately, there is a discontinuity in NO_x emissions when this transition occurs (Morgenstern et al., 2017), which will impact the O_3 trend calculation. **The three sensitivity simulations (SEN-C2-fODS , SEN-C2-fGHG, and SEN-C2-fCH4) differ from the REF-C2 simulation in that ODSs, GHGs, and CH_4, are fixed at their 1960 levels, respectively.** The discontinuity in NO_x emissions exists in all three sensitivity simulations, therefore, we anticipate that its effect will be similar across all simulations. We analyse results from 1987 to 2014, which cover the Lauder ozonesonde time series. The time evolutions of CH_4, CO_2, N_2O, Cl_y, and Br_y, and the surface emissions of NO_x and CO are displayed in Fig. 1.

3 Observed ozone variabilities and trends at Southern Hemisphere mid-latitudes

3.1 Ozone variability

Deseasonalised O_3 anomalies, based on observed O_3 at Lauder, at the eight layers from the surface to the lower stratosphere, and the respective regressed O_3 anomalies are shown in Fig. 2. The observed monthly mean data was generated by performing a linear regression through the observed O_3 sonde data taken during each month (normally 3 or 4 measurements), to define a representative point in the middle of the month. The regressed O_3 values are generated based on the monthly mean observed data via the multi-linear regression expressed by equation 1. O_3 anomalies shown in Fig. 2 and in subsequent figures, where indicated in respective figure captions, are smoothed with a 13-month filter for the purpose of display. Fig. 2 shows that large interannual variations exist in the observed O_3 anomalies, and the O_3 regression captures much of the variability in the stratosphere, but is less accurate at capturing variations in tropospheric O_3 in general (Fig. 2). The amount of O_3 variance explained by the regression is given by the multiple regression coefficient of determination, R^2 (Fig. 2 and Table 2), which shows that in the layer of 9-12 km, the regression achieves the highest

R^2 value of 0.55, followed by the lower stratospheric layers (12-20 km) with R^2 values of 0.38 and 0.36, respectively. The surface layer has a better fit (R^2 = 0.32) than the layers in the free tropospheric layers which have lower R^2 values of 0.08-0.28.

We show contributions of individual regression functions to the regressed O_3 anomalies (Fig. 3) and identify major contributing variables measured by the coefficient determination of individual regression functions, r^2 (Table 2). At the surface, the O_3 anomaly is reasonably well captured by the regression which is dominated by relative humidity (Fig. 3); this may indicate that stratospheric intrusions play a significant role in controlling surface O_3 variations at Lauder, as relative humidity is considered an effective indicator of such intrusions (e.g., Cristofanelli et al., 2006; Stohl et al., 2000). Around and immediately above the tropopause (i.e. 9-15km), the O_3 anomalies largely follow the tropopause height (Fig. 3), which reflects that O_3 in this region is mainly controlled by changes in dynamics. **Indeed, change in tropopause height dominates the regression function at the layer of 9-12 km (r^2 = 0.50), and such dynamical change also influences O_3 variability in the troposphere and the lower stratosphere (see Table 2).** In the free troposphere, between 1.5 km and 9 km, O_3 variations ~~project onto~~**are mostly driven by** a number of factors including tropopause height, relative humidity, **surface temperature**, and the MEI, with **surface temperature and** relative humidity playing a dominant role in the lower troposphere. There is a notable influence of ENSO on ozone variations in the region between 3 and 9 km (Fig. 3). **In the lower stratosphere, stratospheric temperature and the QBO at 30 hPa show increasing dominance in contributing to O_3 variability (Table 2).** ~~Note that when considering regression factors, we do not remove dependencies between variables.~~

Time series of some of the meteorological and climate variables used in the regression are shown in Fig. 4. Except for the MEI time series, all other variables are measured jointly with O_3 at Lauder. ~~Surface temperature is also shown which is not part of the regression function.~~ In order to directly assess the relationship between these variables and O_3 variability, we calculate correlation coefficients (r) of these variables with O_3 anomalies for each layer (see Table 3). This analysis shows clearly that RH_{surf} exhibits a strong anti-correlation with the O_3 anomalies close to the surface ($r = -0.50$), and the correlation reduces at higher altitudes, implying a role for deep stratospheric intrusion in near-surface O_3 variability as mentioned above. Surface temperature anomalies and O_3 anomalies in the troposphere are positively correlated, but are anti-correlated in the stratosphere. Likewise, stratospheric temperature anomalies and stratospheric O_3 anomalies are correlated. **Tropopause height and O_3 are anti-correlated in the stratosphere and are correlated in the troposphere, and the strongest anti-correlation occurs in the tropopause region (9-12 km; $r = -0.71$) and immediately above the tropopause (12-15 km; $r = -0.57$). Moderately high correlation coefficients are calculated between tropopause height and O_3 anomalies in the free troposphere and in the lower stratosphere, indicating the predominant impact of dynamical changes on O_3 over Lauder.** There are rather weak correlations between ENSO (expressed as MEI) and O_3 anomalies, with the largest influence from ENSO in the free troposphere at this mid-latitude location. QBO at 30 hPa is mostly anti-correlated with ozone anomalies in the stratosphere.

Significant correlations exist between some regression functions, e.g., surface temperature and surface relative humidity ($r = -0.41$), tropopause height and surface temperature ($r = 0.50$), tropopause height and stratospheric temperature ($r = -0.28$), and surface temperature and stratospheric temperature ($r = -0.23$), therefore it is expected that

increased uncertainties exist in the combined use of these variables in regression. In this study, however, variables with dominant contributions to the regression function (listed in Table 2) are all significant at the 95% confidence level.

3.2 Ozone trends

The linear trends in observed deseasonalised O_3 anomalies calculated for each layer are listed in Table 4, and are also shown in Fig. 2. Significant positive linear trends (0.04 ppbv/yr) are found from the surface up to 6 km over the 28 year period (1987 to 2014). No significant trend is calculated for 6-9 km. Above 9 km, trends become significantly negative, but with an insignificant negative trend obtained for 20-25 km. To examine if there are any synergies between the trends in O_3 and the dominant meteorological and climate variables, the linear trends of the meteorological and climate variables over this period are also calculated and are shown in Fig. 4; it clearly shows that there are significant linear trends in MEI, RH_{surf}, surface and stratospheric temperatures, and tropopause height anomalies over the period of 1987 to 2014, with significant positive trends in surface temperature (0.02$\pm$0.01K/yr), and the tropopause height (17.9$\pm$5.5 m/yr), and significant negative trends in RH_{surf} (-0.25$\pm$0.06%/yr), stratospheric temperatures (-0.13$\pm$0.01K/yr), and MEI (-0.03$\pm$0.01/yr) (Fig. 4). Significant trends in these variables may indicate some shifts in climate variability, and climate change, which are mainly induced by increasing GHGs (e.g., Mitchell et al., 1995; Santer et al., 1996). Indeed, the increase in surface temperature and the large decrease in stratospheric temperature are the result of a modified radiation balance. Temperature changes in turn result in dynamical changes, such as changes in tropopause height as shown in Fig. 4, likely due to stratospheric cooling. RH_{surf} shows a significantly strong negative trend; this is typically linked to increased deep stratospheric intrusion. MEI shows a moderate negative trend which can be explained by a shift in climate variability. We also calculate O_3 trends over the period of 1987 to 2010, and obtain slightly larger significant positive O_3 trends in the troposphere (Table 4) than those from the period of 1987 to 2014.

Our trend calculation is in broad agreement with Oltmans et al. (2013), who calculated a trend of 0.15 ppbv/yr in O_3 from the surface to the free troposphere over the period of 1986-2010, and no significant trend above 500 hPa, although they did not include O_3 trends in the stratosphere in their study. Oltmans et al. (2013) did not elaborate on what exactly drives the significant positive trends in the lower troposphere at the SH mid-latitude site Lauder. There is no significant trend in the upper troposphere. They suggested that such a pattern in tropospheric O_3 trends does not reflect a possible increase in stratosphere-troposphere exchange (STE), as increasing STE would lead to an increase in O_3 in the upper and free troposphere. From our analysis based on regression/correlation, the deep stratospheric intrusions may play a role in the lower tropospheric O_3 trends, reflected in the significant negative trend in relative humidity over the period of 1987 to 2014 (Fig. 4). However, we cannot derive simple and direct links between changes in relative humidity, deep stratospheric intrusions, and the observed trends in near-surface O_3. In the tropopause region, the change in tropopause height clearly drives the O_3 variation and trend, i.e., significant upward trends in tropopause height imply significant negative O_3 trends between 9 to 15 km (Figs. 2 and 4). In the stratosphere above 15 km, **negative O_3 trends become weaker and are not significant at the 95% confidence level. Long-term changes in O_3 in this region are influenced by changes in dynamics (which are reflected in changes in stratospheric temperatures linked to O_3 changes), and O_3 depletion/recovery that is governed by changes in O_3 depleting substances;**

such changes seem to have cancelled out the decrease in O_3 resulting from the tropopause height increase in this region. Similarly, the insignificant trend in O_3 between 6 and 9 km may be the result of cancellations between the increase of O_3 in the lower troposphere and the decrease of O_3 in the tropopause region. In Sect. 4, we analyse a set of sensitivity simulations designed to assess the contributions from some anthropogenic forcings (ODSs, GHGs, and O_3 precursors), that are known to have caused substantial changes in recent decades to O_3 trends.

3.3 Baring Head surface O_3

In addition to the ozonesonde record at Lauder, we examine the surface O_3 time series from Baring Head (41.4S, 174.9E, 85m) which is also a SH mid-latitude background station located in central New Zealand. In southerly wind situations Baring Head, a coastal site, is exposed to clean marine air. The surface O_3 measurements at Baring Head started in 1991; the record is largely continuous except for some missing data in 2005. The surface O_3 measurements have been made using ultraviolet (UV) photometric ozone analysers (Dasibi model 1003-PC from 1991-2004, and Thermo Electric Corporation TEI49i from 1995), with air drawn from 5 metres above the ground through a dedicated teflon tube with a 0.5 μ teflon filter on the inlet to exclude aerosols. Hourly data from 1992 to 2015 are used to calculated the surface O_3 anomaly and the trend. The data are also deseasonalised.

Shown in Fig. 5, a significant positive trend is calculated in surface O_3 (0.057 ppbv year^{-1}) at Baring Head, which is similar to the trend found at Lauder (0.04$-$0.06 ppbv year^{-1}), but the positive trend calculated from near-surface ozonesonde data at Lauder exhibits a much larger uncertainty range. The significant positive trend in surface O_3 at Baring Head, together with the significant positive trends in Cape Grim and Cape Point surface O_3 calculated by Oltmans et al. (2013), confirms that the positive surface O_3 trends in the SH mid-latitudes are robust. The insignificant positive trend in surface O_3 at Baring Head calculated by Oltmans et al. (2013) over the period of 1991-2010 is due to the shorter data record compared to the record used here.

4 Attribution of ozone trends using chemistry-climate model simulations

4.1 Modelled ozone trends at Lauder

In order to attribute the observed O_3 trends at Lauder in a more quantitative way, we compare the observations to model results. Although the model has a relatively coarse resolution, the measurement site is representative of SH mid-latitudes which are characterized by relatively large-scale variability in O_3. Firstly, we show in Fig. 6 **monthly mean** O_3 volume mixing ratios at all eight layers, for both REF-C1 and REF-C2 simulations (in the case of REF-C1, the run ends in 2010, therefore we use the period of 1987-2010). The model data are interpolated to the vertical resolution of the ozonesonde, before being grouped into the same eight layers as defined before. Overall, the model captures the magnitude and variability of O_3 well, albeit with the overestimation of some observed peak values, mainly at the surface and in the stratosphere. The model is capable of reproducing the observed O_3 seasonal cycle in general, but underestimates the O_3 seasonal cycle in the free troposphere at this

location. Comparing the two model experiments, i.e. REF-C1 and REF-C2, O_3 values in the REF-C1 experiment are generally larger than those in REF-C2, with the largest differences in the free troposphere at 3-6 km. Such differences might be due to the dynamical differences arising from differences in sea surface temperatures between the two experiments. We calculate the linear trends of O_3 in both experiments, and in the sensitivity experiments. The results are discussed in the following sections.

4.2 REF-C1 simulation and the impact from O_3 precursor emissions and the stratosphere

Layer-resolved O_3 anomalies and their trends from REF-C1 and SEN-C1-fEMIS are displayed in Fig. 7 for the period of 1987-2010, together with the observed anomalies for the same period. **Modelled O_3 anomalies are based on monthly mean output from the CCMs, smoothed using a 13-months filter. Trends are calculated based on monthly mean data without any smoothing. The same applies for all modelled O_3 anomalies shown in respective figures.** In addition, the anomalies in the stratospheric O_3 tracer O_3S are also displayed in the same plot. ~~Note that modelled O_3 anomalies are also calculated based on monthly mean data, as applied to the observed anomalies.~~ The modelled trends of O_3 and O_3S are summarised in Table 4. Overall, the REF-C1 simulation captures some basic observed variability but misses some large anomaly features, for example, the very negative O_3 anomalies near the surface in the year 2000, and at the beginning of the record (1987-1988). There are large observed variations in the upper troposphere (6-9 km) that the model fails to reproduce. The observed variabilities of O_3 around the tropopause and in the lower stratosphere are well captured by the model. The modelled trends match well with the observed trend in the tropopause region and in the upper troposphere (6-12 km), but the model cannot reproduce the observed significant positive O_3 trends below 6km. The model simulation also produces a positive, but smaller than observed, trend in **tropopause height (7.6$\pm$3.7 m/year over 1987-2010**. Above 15 km in the stratosphere, large positive anomalies from the model at the beginning of the record are opposite in sign to the observed negative anomalies, and lead to the significant negative trends calculated in the REF-C1 simulation **(excluding the first few years of data, e.g., 1987-1989, the model will produce a weaker insignificant negative trend at 20-25 km)**. In contrast, observed O_3 trends in the stratosphere are generally insignificant. **For comparing to observations at a specific location, we expect that chemical transport models (CTMs) or CCMs with specified dynamics (CCM-SD) would be more accurate in capturing the O_3 variability and other dynamical variables than free-running CCMs; this has been demonstrated in previous studies (e.g., Hardiman et al., 2017). This could have implications for prejecting long-term future O_3 trends using free-running CCMs. Therefore, careful evaluations of free-running CCMs are needed. However, Hardiman et al. (2017) also find that tropical upwelling and the stratospheric meridional circulation are difficult to constrain and are worse in the nudged simulations than in the free-running simulations. Here, we aim to attribute observed O_3 trends to various chemical and dynamical processes, and consider that free-running CCMs are the more suitable models to be used in such study.**

We consider the REF-C1 simulation to be a representation of the realistic O_3 evolution, driven by observed SSTs and well-understood historic anthropogenic forcings such as GHGs and ODSs, including CH_4 which affects O_3 in both chemically and as a GHG. However, anthropogenic non-methane O_3 precursors have relatively large uncertainties, due to their very heterogeneous distributions and poorly understood emission inventories over some parts of the world. SEN-C1-fEMISS is designed to assess how such uncertainties in anthropogenic emissions of non-methane O_3 precursors might affect the O_3 evolution. We take the

results of SEN-C1-fEMISS from 1987 to 2010, and display the anomaly and trend of O_3 in the same manner as O_3 from the REF-C1 simulation (Fig. 7). The comparison shows that there is no apparent difference between O_3 trends in the troposphere between these two simulations, but there are distinct differences from the tropopause region to 25 km. However, the very high REF-C1 O_3 anomalies at the beginning of the record might contribute in part to the very negative trends in the stratosphere. The response of O_3 trend to changing non-methane O_3 precursors is quantified and shown in Table 5. Overall, the non-methane O_3 precursor emission changes between the late 1980s and 2010 have no significant effects on tropospheric O_3 trends, whereas in the stratosphere, the simulation with constant emissions show flat or slightly negative trends in O_3, which indicates changes in emissions (both NO_x and CO surface emissions show global increases during this period; Fig. 1, and Fig. 1 in Morgenstern et al. (2017)) contribute to the negative trends in stratospheric O_3.

The stratospheric tracer O_3S depicted in Fig. 7 shows a weak but significant negative trend near the surface (Table 4). This decrease is likely the result of a decrease in stratospheric O_3 over this period. O_3S is a measure of O_3 originating from the stratosphere, and the negative trend in O_3S also implies that the photochemical production of O_3 in the lower troposphere is increasing, most likely as a result of increasing O_3 precursors including methane. We mentioned before that there seems to be an increase in deep stratospheric intrusion at Lauder over the period of 1987-2014, as indicated by a negative trend in relative humidity. Clearly, STE plays an important role also in controlling lower tropospheric O_3, but a more rigorous attribution of the trend in near-surface O_3 would require a more dedicated set of model experiments, which might be a worthwhile topic of future research.

4.3 REF-C2 simulation and the impact from ODSs, GHGs, and CH_4

In Fig. 8, we compare O_3 anomalies and their trends from the REF-C2 simulations to those from observations for the period of 1987-2014. The variations of observed O_3 anomalies are less accurately matched by the REF-C2 simulations, which are free-running simulations not constrained by observed sea surface conditions, as opposed to the REF-C1 simulations which are driven by observed sea surface conditions. Significant negative trends in O_3 anomalies are calculated for the tropospheric layers, which are neither reflected in the observed trends nor in the REF-C1 simulations which yield a flat trend in the troposphere (Fig. 7). The significant negative tropospheric O_3 trends in REF-C2 are most likely the consequence of a sharp drop in surface NO_x emissions after the year 2000 in the REF-C2 simulations, due to adopting a different emission dataset in 2000 (RCP6.0) that differs from the MACCity emission inventory used in REF-C1 (see Fig. 1 and a related discussion in Morgenstern et al., 2017). This discrepancy in NO_x emissions between REF-C1 and REF-C2 simulations results in significant differences in modelled O_3 trends at Lauder, a background SH mid-latitude site, indicating the important role of surface emissions of O_3 precursors impacting SH O_3 trends, most likely through inter-hemispheric transport. However, around the tropopause and in the stratosphere, the REF-C2 simulation reproduces the observed O_3 trends, in contrast to the REF-C1 simulations, although the variations in observed O_3 are less well reproduced in REF-C2 than in REF-C1.

The purpose of using REF-C2 and SEN-C2 simulations is to assess the role of key forcing agents (ODSs, GHGs, and CH_4) in affecting the long term O_3 trend. In Fig. 8, we also display the O_3 trends from the sensitivity runs. For fixed-ODSs run (i.e. SEN-C2-fODS), the negative trends in O_3 are smaller in magnitudes than those from REF-C2 in the troposphere, which

indicates that changes (i.e. increases) in ODSs between 1987 and 2015 would decrease the tropospheric O_3. However, there is no significant difference in trends between REF-C2 and SEN-C2-fODS simulations in the stratosphere. Halogen loading in the atmosphere (Fig. 1) peaked in the 1990s and then dropped gradually approximately to the late-1980s level in 2014. This could explain the relatively small overall impact from ODSs over the period of 1987-2014 on O_3 at Lauder. The negative impact of ODSs changes during this period on tropospheric O_3 is also reflected in the O_3S tracer which shows a small but significant negative trend over this period (Fig. 7). Changes in GHGs over the period of 1987-2014 produce a negligible impact on simulated tropospheric O_3 changes at Lauder, but have significant impact on trends in stratospheric O_3 (above 12 km) (Fig. 8). The significant negative trends of O_3 in the fixed-GHGs simulations in the stratosphere imply increases in GHGs over 1987-2015 would contribute positively to the stratospheric O_3 trends. The effect is due to changes in CO_2, CH_4, and N_2O collectively. We also performed a sensitivity simulation (SEN-C2-fCH_4) with only CH_4 fixed at the 1960 level, to separate the effect of CH_4 from other GHGs, e.g., CO_2 and N_2O. CH_4 is an O_3 precursor and also a GHG (see above). This analysis shows that in SEN-C2-fCH_4, significant negative trends in O_3 are calculated throughout the troposphere, as shown in Fig. 8, indicating that the increase in CH_4 over the period of 1987-2015 contributes positively to tropospheric O_3 trends. Given very similar O_3 trends in the REF-C2 and SEN-C2-fGHG simulations, it implies that increases in CO_2 and N_2O would make negligible or slightly negative contributions to the O_3 trends over this period, out-weighing the positive contribution of increasing CH_4. In the stratosphere, CH_4 through changes in chemistry plays a much less significant role in O_3 trends.

Note that the period analysed (1987-2014) is relatively short, and the overall changes in ODSs and GHGs (including CH_4) are relatively small. Consequently, changes in O_3 trends attributable to these climate/chemical forcings are usually associated with large uncertainties , and therefore not significant at 95% confidence level (Table 5). Overall, changes in CH_4 contribute positively to tropospheric O_3 trends through enhanced photochemical production of O_3. Increases in GHGs alone seem to result in decreasing tropospheric O_3 (presumably via enhanced chemical destruction in a future warmer and wetter climate) although this is counter balanced by increasing tropospheric O_3 through CH_4 oxidation. Increasing ODSs lead to significant negative O_3 trend in the troposphere, through downward transport of stratospheric O_3. In the stratosphere, the effect from ODSs is small due to the overall small changes in ODS over this period, whilst increases in GHGs seem to be the major forcing, contributing positively to stratospheric O_3 trends through, possibly, decelerated O_3 destruction due to cooling. This positive contribution may have outweighed any reduction of stratospheric O_3 resulting from negative O_3 trends that is triggered by dynamical changes in the tropopause region, as both observations and REF-C2 simulations show relatively small and insignificant trends in stratospheric O_3 at Lauder. In the tropopause region, O_3 trends are not sensitive to changes in these forcings, and are largely controlled by dynamical changes, e.g., the movement of the tropopause. Both REF-C1 and REF-C2 produce a positive, albeit smaller than observed, trend in tropopause height, which agrees with the scientific finding that anthropogenic forcings, in particular O_3 and well-mixed GHGs changes, contribute predominantly to observed tropopause height increase in recent decades (e.g., Santer et al., 2003).

In the following section, we expand the analysis to include the whole simulation period of 1960-2010, and assess long-term simulated changes in O_3 at SH mid-latitudes (represented by Lauder) due to changes in anthropogenic forcings of ODS, GHGs, and O_3 precursor emissions.

4.4 Modelled attribution to long-term O_3 changes at Lauder

Figures 9 and 10 display the O_3 evolution and trends over the 1960-2010 period from REF-C1 and REF-C2, respectively, and the associated sensitivity simulations. The O_3 anomalies are all normalised to zero at the starting time point. The analysis shows that in both simulations, O_3 shows insignificant or moderately negative trends in the troposphere, and more significant negative trends in the stratosphere (Table 6). **It should be noted that larger negative trends in stratospheric O_3 are simulated in REF-C1 than those in REF-fC2; there are sustained stratospheric O_3 losses prior to the 1980s in REF-C1, which are not present in REF-C2 simulations. Relative to the period of Lauder O_3 sonde observations, both simulations show stratospheric O_3 losses from the 1980s to around 2000, and then O_3 recovery after the year 2000 (Figures. 9 and 10), although such changes are not obvious in observed lower stratospheric O_3 at Lauder because of large variability (Figures 7 and 8).**

Examining the sensitivity simulation SEN-C1-fEMIS, fixing emissions at the 1960 level results in negative trends throughout the domain, but with larger negative trends in the troposphere and smaller negative trends in the stratosphere, compared to REF-C1. This means that increases in O_3 precursor emissions since the 1960s lead to a positive contribution to tropospheric O_3 (shown in Fig. 9), predominantly through increased chemical O_3 production. **However, increases in O_3 precursor emissions cause a reduction in stratospheric O_3; we can only suspect that this is due to chemical and/or dynamical changes in the lower stratosphere as a result of O_3 feedback, and this warrants further investigation**. In the tropopause region (9-12 km), the impact on O_3 trends from fixed emissions is minimal, **which may suggest that** changes in O_3 at the tropopause are mainly controlled by the movement of the tropopause rather than **changes in O_3 precursors in the troposphere, and indeed, our calculation shows that there is no significant difference in modelled tropopause heights between SEN-C1-fEMIS and REF-C1 simulations**. In addition, the stratospheric tracer O_3S from REF-C1 is also shown, which shows negative trends, as a result of the declining stratospheric O_3 during this period.

In the fixed-ODSs simulations, large differences in O_3 trends from the correspondent O_3 trends in REF-C2 are shown (Fig. 10), indicating significant negative contributions to O_3 trends due to changes (i.e. increases) in ODSs between 1960 and 2010. By comparison, changes in GHGs seem to have less impact on O_3 trends than ODSs changes. **Increases** in GHGs generally contribute positively to O_3 trends over this period, and the largest influence occurs in the troposphere, whereas the impact on stratospheric O_3 trends is negligible. Interestingly, the impact of changing GHGs on O_3 trends is shown mainly through CH_4 changes, suggesting that chemical changes (O_3 production through increased CH_4) are likely to dominate the contribution of changing GHGs to O_3 trends, especially given that the contribution mainly occurs in the troposphere (Fig. 10). We can not identify in this study the role of individual GHGs in moderating O_3 trends, and it is possible that radiative feedbacks are different from different GHGs, and chemical feedbacks also differ, e.g., CH_4 contributes to O_3 chemical production and N_2O plays a role in stratospheric O_3 destruction. The attribution of modelled O_3 trends to each of the aforementioned forcings is listed in Table 6.

5 Conclusions

We have analysed a 28-year ozonesonde record from Lauder, covering 1987 to 2014, and a surface O_3 record from Baring Head covering 1992 to 2015. Both background measurement sites are located in the SH mid-latitudes, and are representative of background atmospheric conditions. We have also analysed some meteorological parameters that are co-measured with O_3 at Lauder, and have explored the relationships between O_3 changes and changes in these parameters, i.e., surface relative humidity, surface and stratospheric temperatures, and tropopause height, respectively. Through a regression analysis of ozonesonde data, which involves grouping the profiles into eight layers extending to the stratosphere (25 km), we have identified the dominant meteorological parameters that control the interannual variations of O_3 at Lauder. We find that relative humidity dominates the variability of lower tropospheric O_3, possibly through deep stratospheric intrusions, and that O_3 variability around the tropopause region is dominated by the movement of the tropopause. In addition, ENSO contributes to O_3 variations in the free troposphere, and the QBO and solar cycle impact O_3 variations in the stratosphere.

The trends in observed O_3 at Lauder have been calculated for the eight layers. Significant positive trends in the troposphere below 6 km, and significant negative trends in the tropopause region are obtained, for both 1987-2010 and 1987-2014. No significant trends are found in the upper troposphere (6-9 km) and in the stratosphere (above 15 km). A significant negative O_3 trend in the 9-12 km region is very likely the result of an increasing tropopause height at Lauder. Such a dynamically induced change in O_3 also propagates to below and above the tropopause. Changes in temperatures in both the troposphere and the stratosphere impact O_3 by modifying the chemical production and destruction rates. Specifically, increased surface temperature would enhance photochemical production of O_3 mainly in the lower troposphere, and decreased stratospheric temperature would slow down the nitrogen- and halogen-catalysed O_3 destruction cycles. Such effects from temperature changes could be balanced by the effect from tropopause height changes; the net impact are small O_3 trends in the upper troposphere and the lower stratosphere.

We have used NIWA-UKCA chemistry-climate model simulations to attribute O_3 trends observed at Lauder to anthropogenic influences, particularly changing GHGs, ODSs, and O_3 precursors over 1987 to 2014. Results from these CCMI simulations indicate that O_3 precursor emissions have no net impact on tropospheric O_3, but lead to significant negative trends in stratospheric O_3; this will be further investigated. Changes in CH_4 generally have a positive impact on O_3, but the effect is not significant at the 95% confidence level. Changes in GHGs (including CH_4) mainly affect the stratosphere where increased GHGs lead to significant positive trends in O_3. Increases in ODSs during this period mainly result in negative O_3 trend in the troposphere, through stratosphere-troposphere exchange and/or consequences for tropospheric ozone photochemistry. But with Br_y and Cl_y peaking in the late 1990s, stratospheric O_3 at Lauder is not significantly affected by overall changes in ODSs from 1987 to 2014. We also examined O_3 transported from the stratosphere using a diagnostic stratospheric O_3 tracer, which shows a significant negative trend near the surface, suggesting that changes in stratosphere-troposphere exchange of ozone are indeed involved in tropospheric ozone trends.

The observed significant positive trend in tropospheric O_3 below 6 km is not reproduced by the base simulations (REF-C1 and REF-C2), which is very likely because of an underestimation of positive trends in surface emissions of O_3 precursors. The

large significant negative trend in stratospheric O_3 in the REF-C1 simulation is caused by the very large positive anomaly at the beginning of O_3 record. Both base simulations reproduce well the significant negative O_3 trend in the tropopause region, associated with dynamical changes.

The Lauder O_3 record presented in this study is relatively short for detecting significant responses of O_3 to changes in GHGs, ODSs, and O_3 precursors. The analysis is extended to cover the whole period of the simulation, i.e., 1960-2010, during which period significant changes in GHGs, ODSs, and O_3 precursors occur, allowing for a more robust assessment of their impacts on the O_3 evolution. The results show that all forcings contribute significantly to simulated O_3 trends over the last five decades at Lauder. Increases in O_3 precursors contribute positively to tropospheric O_3 through enhanced photochemical production of O_3, but negatively to stratospheric O_3. The increase in CH_4 leads to positive O_3 trends in both the troposphere and the stratosphere, and is comparable to the O_3 response to the net effect of combined GHGs changes, indicating there may be a cancellation of effects from increases in CO_2 and in N_2O. The overall increase in ODSs between 1960 and 2010 results in significant negative trend in tropospheric and stratospheric O_3, which coincides with the negative trend in the stratospheric O_3 tracer.

This study demonstrates that long-term ozone profile observations provide valuable insight into atmospheric composition changes associated with anthropogenic forcing over the recent decades at a background SH mid-latitude location. More locations can be explored in future studies and multi-model simulation ensembles can be used to derive global O_3 changes, and to project the future evolution.

Data availability. All data used in this paper can be obtained from the contact author. The Lauder ozonesonde data are available at ftp://ftp.cpc.ncep.noaa.gov/ndacc/station/lauder/ames/o3sonde/. Baring Head surface O_3 data are available at http://ds.data.jma.go.jp/gmd/wdcgg. NIWA-UKCA simulations can be downloaded from the CCMI archive; see instructions at http://blogs.reading.ac.uk/ccmi/badc-data-access/

Competing interests. The authors declare that they have no conflict of interest.

Acknowledgements. We acknowledge the NIWA Lauder Ozone team for ozone sonde measurements since 1986, and technicians involved at various stages of data collection. We acknowledge the U.K. Met Office for use of the MetUM. Furthermore, we acknowledge the contribution of NeSI high-performance computing facilities to the results of this research. NZ's national facilities are provided by the NZ eScience Infrastructure and funded jointly by NeSI's collaborator institutions and through the Ministry of Business, Innovation & Employment's Research Infrastructure programme (https://www.nesi.org.nz). This research was supported by the NZ Government's Strategic Science Investment Fund (SSIF) through the NIWA programmes CACV and CAAC, and by the Marsden Fund Council from New Zealand Government funding, managed by the Royal Society of New Zealand, under project 12NIW006.

References

Beekmann, M., Ancellet, G., and Mégie, G.: Climatology of tropospheric ozone in Southern Europe and its relation to potential vorticity, J. Geophys. Res., 99, 12,841–12,853, 1994.

Bethan, S., Vaughan, G., and Reid, S. J.: A comparison of ozone and thermal tropopause heights and the impact of tropopause definition on quantifying the ozone content of the troposphere, Q. J. R. Meteorol. Soc., 122, 929–944, 1996.

Bodeker, G. E., Boyd, I. S., and Matthews, W. A.: Trends and variability in vertical ozone and temperature profiles measured by ozonesondes at Lauder, New Zealand: 1986 – 1996, J. Geophys. Res., 103, 28,661–28,682, 1998.

Boyd, I. S., Bodeker, G. E., Connor, B. J., Swart, D. P. J., and Brinksma, E. J.: An assessment of ECC ozonesondes operated using 1% and 0.5% KI cathode solutions at Lauder, New Zealand, Geophys. Res. Lett., 25, 2409–2412, 1998.

Cristofanelli, P., Bonasoni, P., Tositti, L., Bonafè, U., Calzolari, F., Evangelisti, F., Sandrini, S., and Stohl, A.: A 6-year analysis of stratospheric intrusions and their influence on ozone at Mt. Cimone (2165 m above sea level), 111, doi:10.1029/2005JD006553, 2006.

Eyring, V., Cionni, I., Bodeker, G. E., Charlton-Perez, A. J., Kinnison, D. E., Scinocca, J. F., Waugh, D. W., Akiyoshi, H., Bekki, S., Chipperfield, M. P., Dameris, M., Dhomse, S., Frith, S. M., Garny, H., Gettelman, A., Kubin, A., Langematz, U., Mancini, E., Marchand, M., Nakamura, T., Oman, L. D., Pawson, S., Pitari, G., Plummer, D. A., Rozanov, E., Shepherd, T. G., Shibata, K., Tian, W., Braesicke, P., Hardiman, S. C., Lamarque, J. F., Morgenstern, O., Smale, D., Pyle, J. A., and Yamashita, Y.: Multi-model assessment of stratospheric ozone return dates and ozone recovery in CCMVal-2 models, 10, 9451–9472, doi:10.5194/acp-10-9451-2010, 2010.

Eyring, V., Lamarque, J.-F., Hess, P., Arfeuille, F., Bowman, K., Chipperfield, M. P., Duncan, B., Fiore, A., Gettelman, A., Giorgetta, M. A., Granier, C., Hegglin, M., Kinnison, D., Kunze, M., Langematz, U., Luo, B., Martin, R., Matthes, K., Newman, P. A., Peter, T., Robock, A., Ryerson, T., Saiz-Lopez, A., Salawitch, R., Schultz, M., Shepherd, T. G., Shindell, D., Staehelin, J., Tegtmeier, S., Thomason, L., Tilmes, S., Vernier, J.-P., Waugh, D., and Young, P. J.: Overview of IGAC/SPARC Chemistry-Climate Model Initiative (CCMI) community simulations in support of upcoming ozone and climate assessments, SPARC Newsletter, 40, 48–66, 2013.

Granier, C., Bessagnet, B., Bond, T., DÁngiola, A., van der Gon, H. D., Frost, G. J., Heil, A., Kaiser, J. W., and Kinne, S.: Evolution of anthropogenic and biomass burning emissions of air pollutants at global and regional scales during the 1980–2010 period, Clim. Change, 109, 163–190, doi:10.1007/s10584-011-0154-1, 2011.

Guenther, A. B., Jiang, X., Heald, C. L., Sakulyanontvittaya, T., Duhl, T., Emmons, L. K., and Wang, X.: The Model of Emissions of Gases and Aerosols from Nature version 2.1 (MEGAN2.1): an extended and updated framework for modeling biogenic emissions, 5, 1471–1492, doi:10.5194/gmd-5-1471-2012, 2012.

Hardiman, S. C., N. Butchart, F. M. O., and Rumbold, S. T.: The Met Office HadGEM3-ES chemistry–climate model: evaluation of stratospheric dynamics and its impact on ozone, 10, 1209–1232, doi:10.5194/gmd-10-1209-2017, 2017.

Hewitt, H. T., Copsey, D., Culverwell, I. D., Harris, C. M., Hill, R. S. R., Keen, A. B., McLaren, A. J., and Hunke, E. C.: Design and implementation of the infrastructure of HadGEM3: the nextgeneration Met Office climate modelling system, Geosci. Model Dev., 4, 223–253, doi:10.5194/gmd-4-223-2011, 2011.

Lary, D. J. and Pyle, J. A.: Diffuse radiation, twilight, and photochemistry- I, 13, 373–392, 1991.

Meinshausen, M., Smith, S. J., Calvin, K., Daniel, J. S., Kainuma, M. L., Lamarque, J.-F., Matsumoto, K., Montzka, S. A., Raper, S. C., Riahi, K., Thomson, A., Velders, G. J., and van Vuuren, D. P.: The RCP greenhouse gas concentrations and their extensions from 1765 to 2300, clim. Chang., 109, 213–241, doi:10.1007/s10584-011-0156-z, 2011.

Mitchell, J. F. B., Johns, T. C., Gregory, J. M., and Tett, S. F. B.: Climate response to increasing levels of greenhouse gases and sulphate aerosols, Nature, 376, 501–504, doi:10.1038/376501a0, 1995.

Morgenstern, O., Braesicke, P., O'Connor, F. M., Bushell, A. C., Johnson, C. E., Osprey, S. M., and Pyle, J. A.: Evaluation of the new UKCA climate-composition model – Part 1: The stratosphere, 2, 43–57, doi:10.5194/gmd-2-43-2009, 2009.

Morgenstern, O., Hegglin, M. I., Rozanov, E., O'Connor, F. M., Abraham, N. L., Akiyoshi, H., Archibald, A. T., Bekki, S., Butchart, N., Chipperfield, M. P., Deushi, M., Dhomse, S. S., Garcia, R. R., Hardiman, S. C., Horowitz, L. W., Jöckel, P., Josse, B., Kinnison, D., Lin, M., Mancini, E., Manyin, M. E., Marchand, M., Marécal, V., Michou, M., Oman, L. D., Pitari, G., Plummer, D. A., Revell, L. E., Saint-Martin, D., Schofield, R., Stenke, A., Stone, K., Sudo, K., Tanaka, T. Y., Tilmes, S., Yamashita, Y., Yoshida, K., and Zeng, G.: Review of the global models used within phase 1 of the Chemistry-Climate Model Initiative (CCMI), 10, 639–671, doi:doi:10.5194/gmd-10-639-2017, 2017.

Neu, J. L., Prather, M. J., and Penner, J. E.: Global atmospheric chemistry: Integrating over fractional cloud cover, 112, doi:10.1029/2006JD008007, 2007.

O'Connor, F. M., Johnson, C. E., Morgenstern, O., Abraham, N. L., Braesicke, P., Dalvi, M., Folberth, G. A., Sanderson, M. G., Telford, P. J., Voulgarakis, A., Young, P. J., Zeng, G., Collins, W. J., and Pyle, J. A.: Evaluation of the new UKCA climate-composition model – Part 2: The Troposphere, 7, 41–91, doi:10.5194/gmd-7-41-2014, 2014.

Oltmans, S., Lefohn, A., Harris, J., Galbally, I., Scheel, H., Bodeker, G., Brunke, E., Claude, H., Tarasick, D., Johnson, B., Simmonds, P., Shadwick, D., Anlauf, K., Hayden, K., Schmidlin, F., Fujimoto, T., Akagi, K., Meyer, C., Nichol, S., Davies, J., Redondas, A., and Cuevas, E.: Long-term changes in tropospheric ozone, 40, 3156–3173, doi:10.1016/j.atmosenv.2006.01.029, 2006.

Oltmans, S. J., Lefohn, A. S., Shadwick, D., Harris, J. M., Scheel, H. E., Galbally, I., Tarasick, D. W., Johnson, B. J., Brunke, E.-G., Claude, H., Zeng, G., Nichol, S., Schmidlin, F., Davies, J., Cuevas, E., Redondas, A., Naoe, H., Nakano, T., and Kawasato, T.: Recent tropospheric ozone changes − A pattern dominated by slow or no growth, 67, 331–351, doi:10.1016/j.atmosenv.2012.10.057, 2013.

Price, C. and Rind, D.: A simple lightning parameterization for calculating global lightning distributions, J. Geophys. Res., 97, 9919–9933, doi:doi:10.1029/92JD00719, 1992.

Price, C. and Rind, D.: Modeling global lightning distributions in a general circulation model, Mon. Wea. Rev., 122, 1930–1939, doi:doi:10.1175/1520-0493, 1994.

Rayner, N. A., Parker, D. E., Horton, E. B., Folland, C. K., Alexander, L. V., Rowell, D. P., Kent, E. C., and Kaplan, A.: Global analyses of sea surface temperature, sea ice, and night marine air temperature since the late nineteenth century, J. Geophys. Res., 108, 4407, doi:10.1029/2002JD002670, 2003.

Santer, B. D., Taylor, K. E., Wigley, T. M. L., Johns, T. C., Jones, P. D., Karoly, D. J., Mitchell, J. F. B., Oort, A. H., Penner, J. E., Ramaswamy, V., Schwarzkopf, M. D., Stouffer, R. J., and Tett, S.: A search for human influences on the thermal structure of the atmosphere, Nature, 382, 39–46, doi:10.1038/382039a0, 1996.

Santer, B. D., Wehner, M. F., Wigley, T. M. L., Sausen, R., Meehl, G. A., Taylor, K. E., Ammann, C., Arblaster, J., Washington, W. M., Boyle, J. S., and Brüggemann, W.: Contributions of Anthropogenic and Natural Forcing to Recent Tropopause Height Changes, Science, 301, 479–483, doi:10.1126/science.1084123, 2003.

Stohl, A., Spichtinger-Rakowsky, N., Bonasoni, P., Feldmann, H., Memmesheimer, M., Scheel, H. E., Trickl, T., Hubener, S., Ringer, W., and Mandl, M.: The influence of stratospheric intrusions on alpine ozone concentrations, pp. 1323–1354, 2000.

Telford, P. J., Abraham, N. L., Archibald, A. T., Braesicke, P., Dalvi, M., Morgenstern, O., O'Connor, F. M., Richards, N. A. D., and Pyle, J. A.: Implementation of the Fast–JX Photolysis scheme (v6.4) into the UKCA component of the MetUM chemistry–climate model (v7.3), 6, 161–177, doi:10.5194/gmd-6-161-2013, 2013.

Thompson, A. M.: The oxidizing capacity of the Earth's atmosphere: Probable past and future changes, Science, 256, 1157–1165, 1992.

Volz, A. and Kley, D.: Evaluation of the Montsouris series of ozone measurements made in the nineteenth century, Nature, 332, 240–242, 1988.

WMO: Scientific Assessment of Ozone Depletion: 2010, Global Ozone Research and Monitoring Project, Geneva, Switzerland, Report No. 52, 2011.

WMO: Scientific Assessment of Ozone Depletion: 2014, Global Ozone Research and Monitoring Project, Geneva, Switzerland, Report No. 55, 2014.

Zeng, G., Pyle, J. A., and Young, P. J.: Impact of climate change on tropospheric ozone and its global budgets, 9, 369–387, doi:10.5194/acp-8-369-2008, 2008.

Zeng, G., Morgenstern, O., Braesicke, P., and Pyle, J. A.: Impact of stratospheric ozone recovery on tropospheric ozone and its budget, Geophys. Res. Lett., 37, L09805, doi:10.1029/2010GL042812, 2010.

Zeng, G., Williams, J. E., Fisher, J. A., Emmons, L. K., Jones, N. B., Morgenstern, O., Robinson, J., Smale, D., Paton-Walsh, C., and Griffith, D. W. T.: Multi-model simulation of CO and HCHO in the Southern Hemisphere: comparison with observations and impact of biogenic emissions, 15, 7217–7245, doi:10.5194/acp-15-7217-2015, 2015.

Table 1. Chemistry-Climate Model Initiative (CCMI) simulations performed by NIWA-UKCA, used in this study.

Simulation	Period	SSTs/sea ice	O_3 precursor Emissions*	CH_4	GHGs*	ODSs
REF-C1	1960-2010	HADISST	MACCity (1960-2010)	RCP 6.0	RCP 6.0	WMO (2014) A1
SEN-C1-fEMIS	1960-2010	HADISST	Fixed at 1960	RCP 6.0	RCP 6.0	WMO (2014) A1
REF-C2	1960-2100	Interactive	MACCity (1960-2000) & RCP 6.0 (2000-2100)	RCP 6.0	RCP 6.0	WMO (2014) A1
SEN-C2-fGHG	1960-2100	Interactive	MACCity (1960-2000) & RCP 6.0 (2000-2100)	Fixed at 1960	Fixed at 1960	WMO (2014) A1
SEN-C2-fCH_4	1960-2100	Interactive	MACCity (1960-2000) & RCP 6.0 (2000-2100)	Fixed at 1960	RCP 6.0	WMO (2014) A1
SEN-C2-fODS	1960-2100	Interactive	MACCity (1960-2000) & RCP 6.0 (2000-2100)	RCP 6.0	RCP 6.0	Fixed at 1960

* Excluding CH_4

Table 2. Coefficient of determination, R^2, and dominant contributors to the regression, based on coefficients of determination of individual regression functions (r^2), resolved by altitude.

Altitudes	R^2	Dominant regression functions (measured by r^2)		
0-1.5 km	0.32	Relative humidity (0.25)	Surface temperature (0.13)	
1.5-3 km	0.21	Tropopause height (0.10)	Surface temperature (0.09)	Relative humidity (0.05)
3-6 km	0.28	Surface temperature (0.15)	Tropopause height (0.11)	Stratospheric temperature (0.08)
6-9 km	0.08	ENSO (0.02)	Tropopause height (0.01)	
9-12 km	0.55	Tropopause height (0.50)	Surface temperature (0.09)	Stratospheric temperature (0.07)
12-15 km	0.38	Tropopause height (0.29)	Surface temperature (0.14)	Stratospheric temperture (0.06)
15-20 km	0.36	Tropopause height (0.14)	Surface temperature (0.11)	QBO at 30 hPa (0.10)
20-25 km	0.35	Stratospheric temperature (0.18)	QBO at 30 hPa (0.09)	Surface temperature (0.03)

Table 3. Correlation coefficients between O_3 anomalies and climate/meteorological variables at each layer.

Ozone layers	RH_{surf}	T_{surf}	T_{strat}	MEI	QBO_{30}	HT_{Trop}
O_3 (0-1.5km)	-0.50	0.38			-0.12	0.16
O_3 (1.5-3km)	-0.28	0.35	-0.17	-0.11		0.34
O_3 (3-6km)	-0.20	0.42	-0.29	-0.18		0.38
O_3 (6-9km)				-0.15		-0.14
O_3 (9-12km)	0.21	-0.44	0.31			-0.71
O_3 (12-15km)	0.23	-0.45	0.27	0.13		-0.57
O_3 (15-20km)		-0.36	0.32	0.10	-0.32	-0.41
O_3 (20-25km)		-0.18	0.43		-0.31	-0.18

Table 4. Observed and simulated trends in O_3 and O_3S anomalies (± 1 Standard Error) at Lauder, over the periods of 1987-2010 and 1987-2014, accordingly. Units are ppbv yr^{-1}.

Altitute/km	Observed O_3	Observed O_3	REF-C1 O_3	REF-C2 O_3	REF-C1 O_3S
	1987-2010	1987-2014	1987-2010	1987-2014	1987-2010
0-1.5	0.06 ± 0.02	0.04 ± 0.01	0.00 ± 0.01	-0.05 ± 0.01	-0.02 ± 0.00
1.5-3	0.08 ± 0.02	0.04 ± 0.01	0.01 ± 0.01	-0.06 ± 0.01	-0.02 ± 0.01
3-6	0.06 ± 0.03	0.05 ± 0.02	0.02 ± 0.02	-0.07 ± 0.01	0.00 ± 0.01
6-9	-0.09 ± 0.05	-0.01 ± 0.05	-0.01 ± 0.02	-0.10 ± 0.02	-0.04 ± 0.02
9-12	-0.55 ± 0.27	-0.62 ± 0.21	-0.39 ± 0.12	-0.26 ± 0.07	-0.47 ± 0.13
12-15	-0.53 ± 0.44	-0.90 ± 0.35	-1.18 ± 0.32	-0.51 ± 0.23	-1.19 ± 0.32
15-20	0.89 ± 1.12	-1.01 ± 0.88	-4.19 ± 0.73	-1.00 ± 0.56	-4.19 ± 0.73
20-25	1.46 ± 1.61	-0.50 ± 1.28	-4.46 ± 0.95	0.20 ± 0.69	-4.56 ± 0.96

Table 5. Attributions of modelled trends (± 1 standard deviation) due to changes in non-methane O_3 precursors (NMOPs), CH_4, GHGs, and ODSs over the period 1987-2010 and 1987-2014, respectively, calculated as trends in absolute differences between O_3 anomalies from the sensitivity simulations and O_3 anomalies from the REF-C1 and REF-C2 simulation, respectively. Units are ppbv yr^{-1}.

Altitude/km	Due to NMOPs	Due to CH_4	Due to GHGs	Due to ODSs
	1987-2010	1987-2014	1987-2014	1987-2014
0-1.5	-0.00 ± 0.01	0.02 ± 0.02	-0.00 ± 0.01	-0.02 ± 0.01
1.5-3	-0.00 ± 0.02	0.02 ± 0.02	-0.00 ± 0.01	-0.03 ± 0.02
3-6	0.02 ± 0.02	0.02 ± 0.02	-0.01 ± 0.02	-0.05 ± 0.02
6-9	0.00 ± 0.03	0.00 ± 0.03	0.00 ± 0.02	-0.08 ± 0.03
9-12	-0.42 ± 0.16	-0.05 ± 0.11	0.20 ± 0.11	0.02 ± 0.12
12-15	-1.05 ± 0.40	0.23 ± 0.51	0.69 ± 0.33	0.14 ± 0.37
15-20	-2.49 ± 0.91	0.50 ± 1.56	1.27 ± 0.79	-0.11 ± 0.92
20-25	-3.20 ± 1.24	1.80 ± 1.99	3.91 ± 1.01	0.52 ± 1.09

Table 6. Simulated trends in O_3 and O_3S anomalies (± 1 standard deviation) at Lauder, and attributions of modelled trends due to changes in non-methane O_3 precursors, CH_4, GHGs, and ODS over the period of 1960-2010. Units are ppbv yr^{-1}.

Altitude/km	REF-C1	REF-C2	Due to NMOPs	Due to CH_4	Due to GHGs	Due to ODSs	O_3S (REF-C1)
0-1.5	0.00 ± 0.00	-0.02 ± 0.00	0.02 ± 0.01	0.03 ± 0.01	0.03 ± 0.01	-0.07 ± 0.01	-0.04 ± 0.00
1.5-3	0.00 ± 0.00	-0.02 ± 0.00	0.02 ± 0.01	0.04 ± 0.01	0.04 ± 0.01	-0.09 ± 0.01	-0.05 ± 0.00
3-6	0.00 ± 0.01	-0.03 ± 0.01	0.03 ± 0.01	0.05 ± 0.01	0.05 ± 0.01	-0.11 ± 0.01	-0.05 ± 0.00
6-9	-0.05 ± 0.01	-0.04 ± 0.01	0.04 ± 0.01	0.05 ± 0.01	0.06 ± 0.01	-0.16 ± 0.01	-0.12 ± 0.01
9-12	-0.51 ± 0.05	-0.26 ± 0.04	-0.26 ± 0.06	0.06 ± 0.05	0.05 ± 0.05	-0.49 ± 0.05	-0.60 ± 0.05
12-15	-1.33 ± 0.13	-0.80 ± 0.11	-0.29 ± 0.15	0.33 ± 0.16	0.29 ± 0.16	-1.24 ± 0.16	-1.33 ± 0.13
15-20	-5.12 ± 0.26	-3.95 ± 0.26	-1.68 ± 0.33	0.49 ± 0.39	0.42 ± 0.38	-4.05 ± 0.38	-5.12 ± 0.26
20-25	-7.88 ± 0.31	-6.25 ± 0.34	-2.51 ± 0.41	0.81 ± 0.48	0.77 ± 0.45	-6.93 ± 0.47	-7.88 ± 0.31

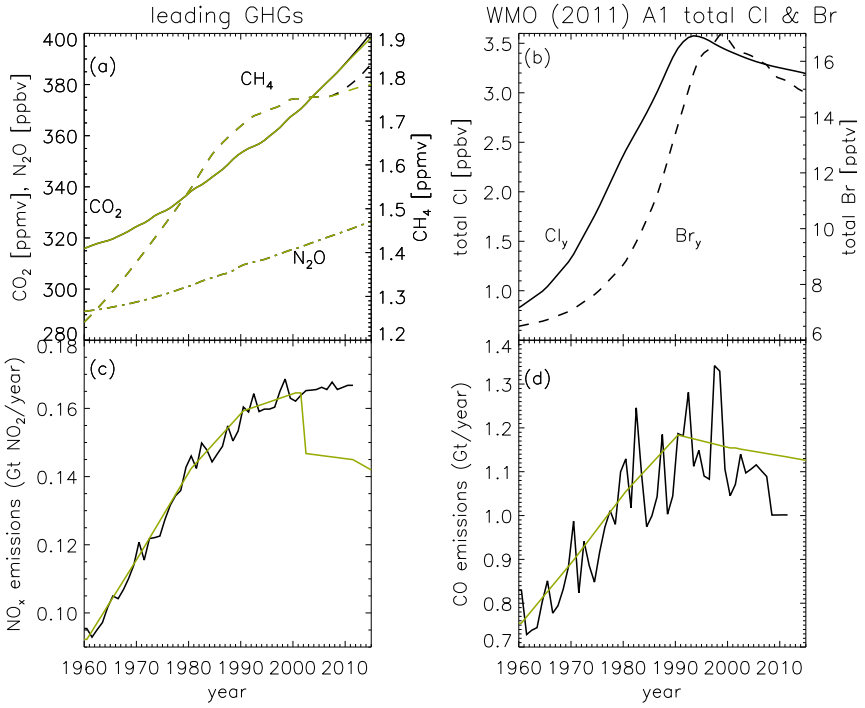

Figure 1. Time evolution of anthropogenic forcings used in CCMI simulations: (a) greenhouse gases (GHGs) volume mixing ratios, (b) total organic chlorine and bromine volume mixing ratios, (c) nitrogen oxides emissions (NO_x), and (d) carbon monoxide emissions (CO). Black lines denote forcings used in REF-C1, and lime lines for REF-C2. Note the discontinuity in NO_x emissions (panel c) mentioned in the text.

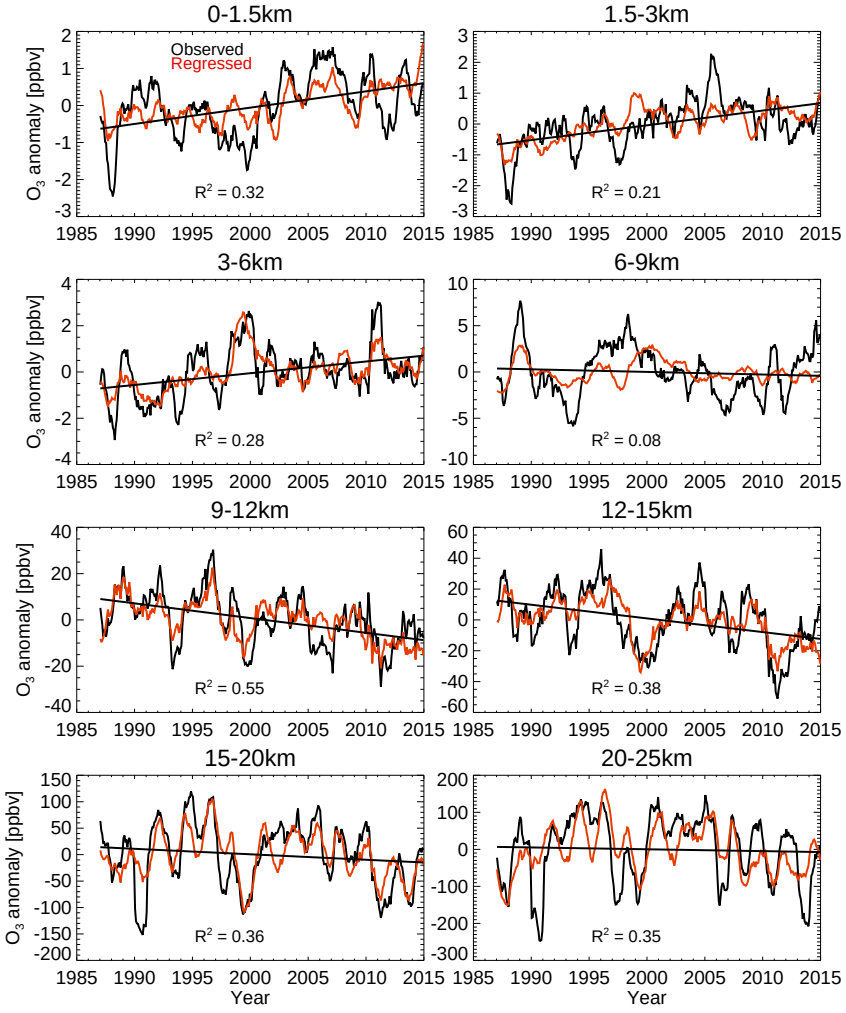

Figure 2. Vertically resolved observed ozone anomalies (black curves), linear trends (black lines), and regressed O_3 anomalies (red curves) at Lauder (1987-2014). R^2 is the coefficient of determination of multi-variant regression function at each layer. The O_3 anmalies shown are smoothed using a 13-month filter based on monthly mean data. Linear trends are calculated from the monthly mean O_3 anomalies.

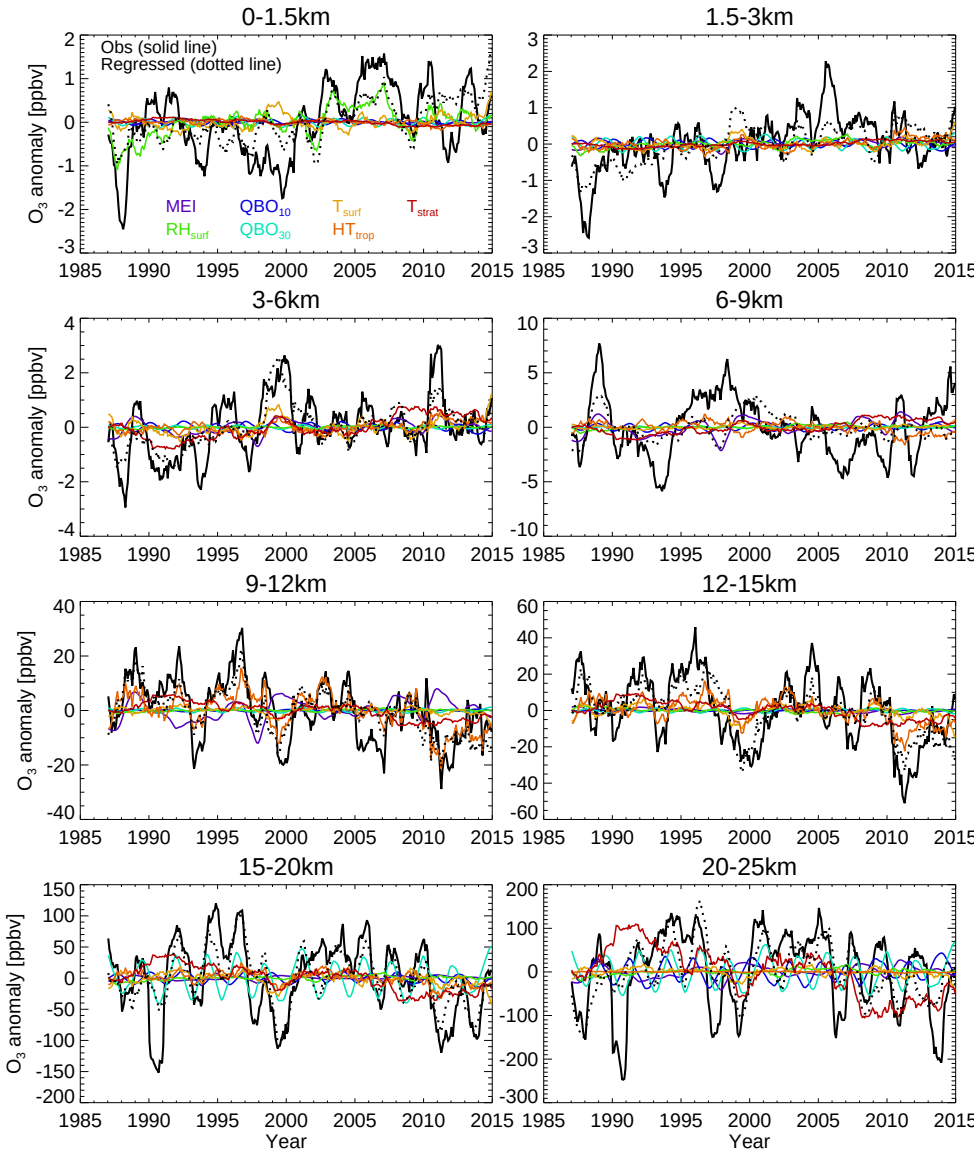

Figure 3. Ozone anomalies and contributions of individual regression functions at Lauder. O_3 anomalies are monthly mean but are smoothed using a 13-month filter for display. Colour keys for regressors are shown in the top-left panel.

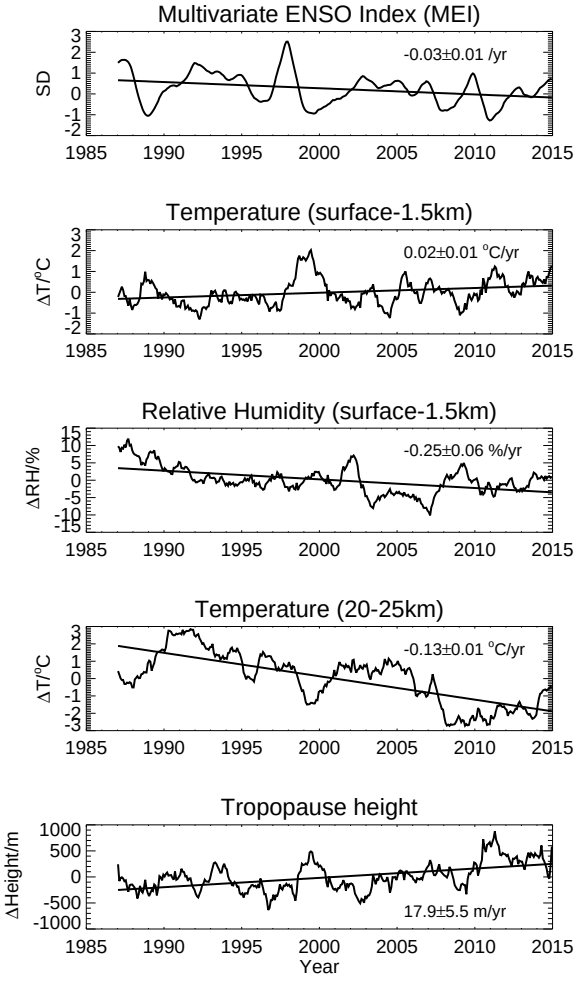

Figure 4. Time series of dominant climate/meteorological variables, co-measured with O_3 at Lauder, with the exception of the ENSO Index (MEI). Anomalies are monthly mean but are smoothed using a 13-month filter for display. Linear trends for all variables are noted in the figure.

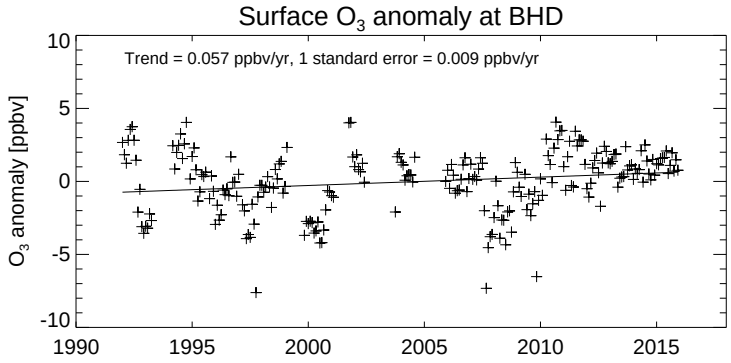

Figure 5. Observed monthly mean surface O_3 anomaly and the corresponding linear trend at Baring Head (1994-2015).

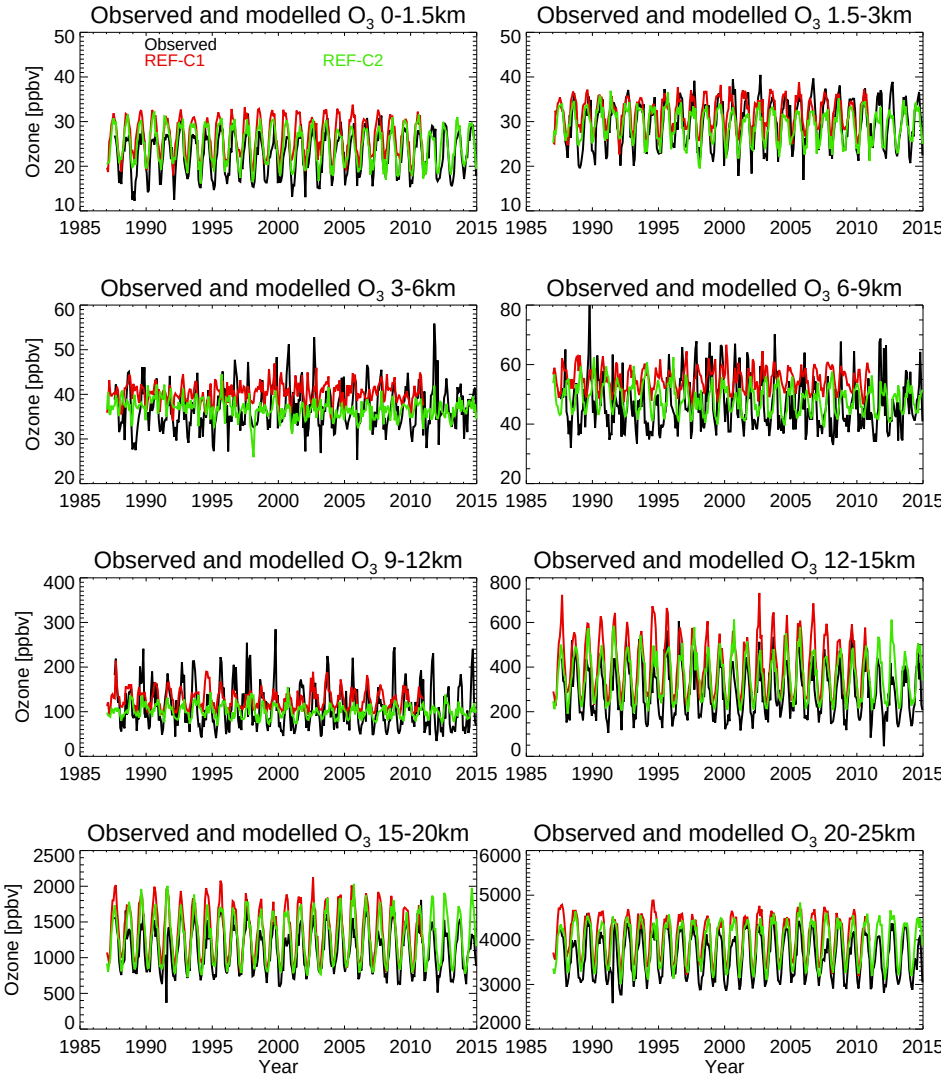

Figure 6. Observed (black) and modelled monthly mean O_3 time series, from REF-C1 (red) and REF-C2 (green) respectively, at Lauder over 1987-2014.The REF-C1 simulation ends in year 2010.

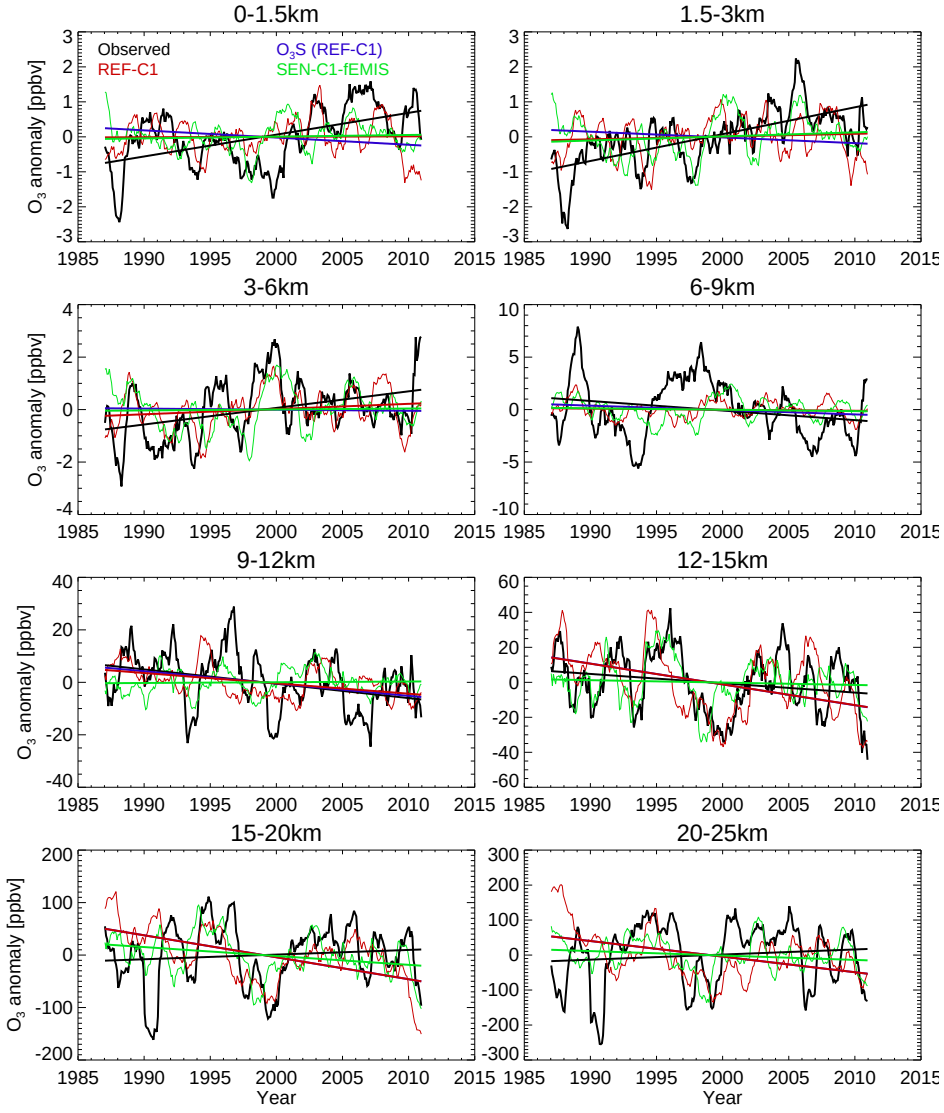

Figure 7. Observed (black) and modelled O_3 anomalies and corresponding linear trends, from REF-C1 (red) and REF-C2 (green) respectively, at Lauder (1987-2010), and the linear trend in O_3S (blue line) from REF-C1. Anomalies shown are smoothed with a 13-monthly filter for the purpose of display.

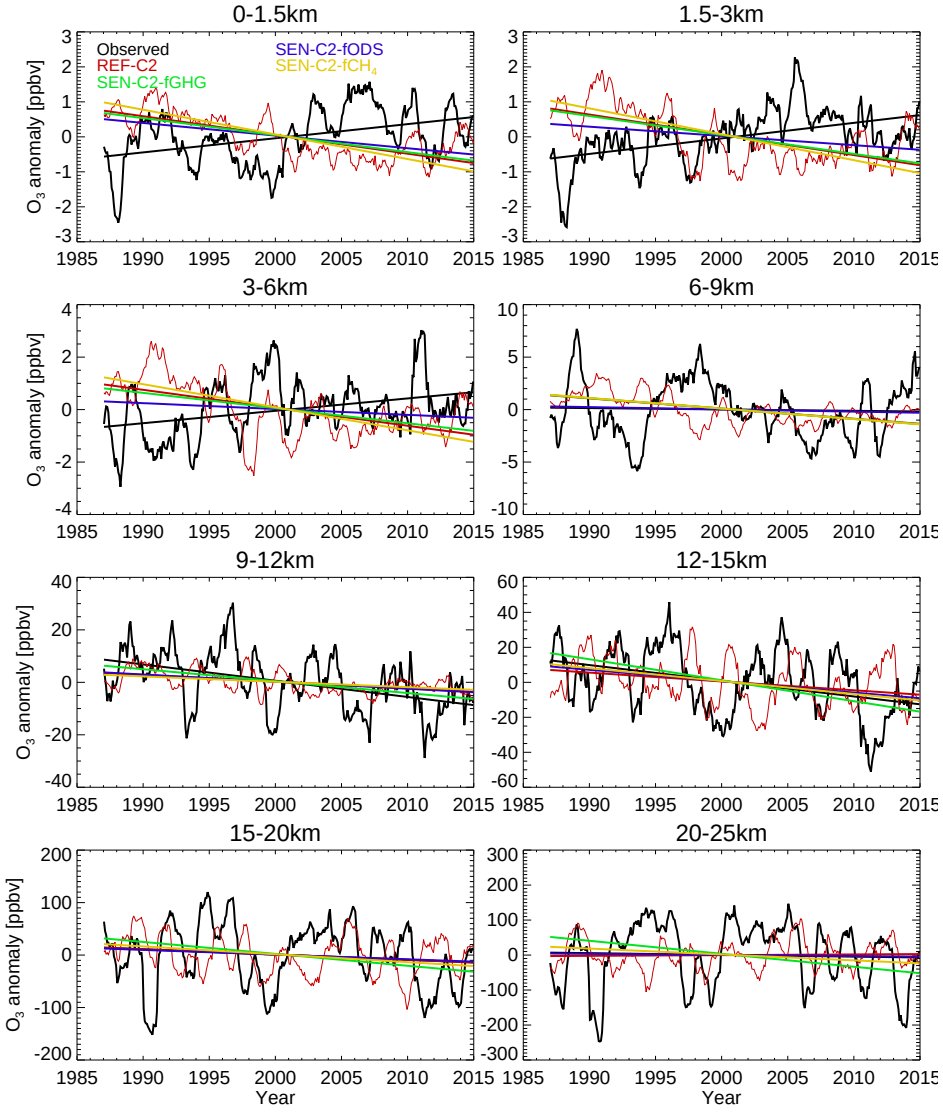

Figure 8. Observed (black) and modelled (REF-C2; red) O_3 anomalies and linear trends at Lauder over 1987-2014. Modelled linear trends from SEN-C2-fGHG (green line), SEN-C2-fCH_4 (gold line), and SEN-C2-fODS (blue line), respectively, are also depicted. Anomalies shown are smoothed with a 13-monthly filter for the purpose of display.

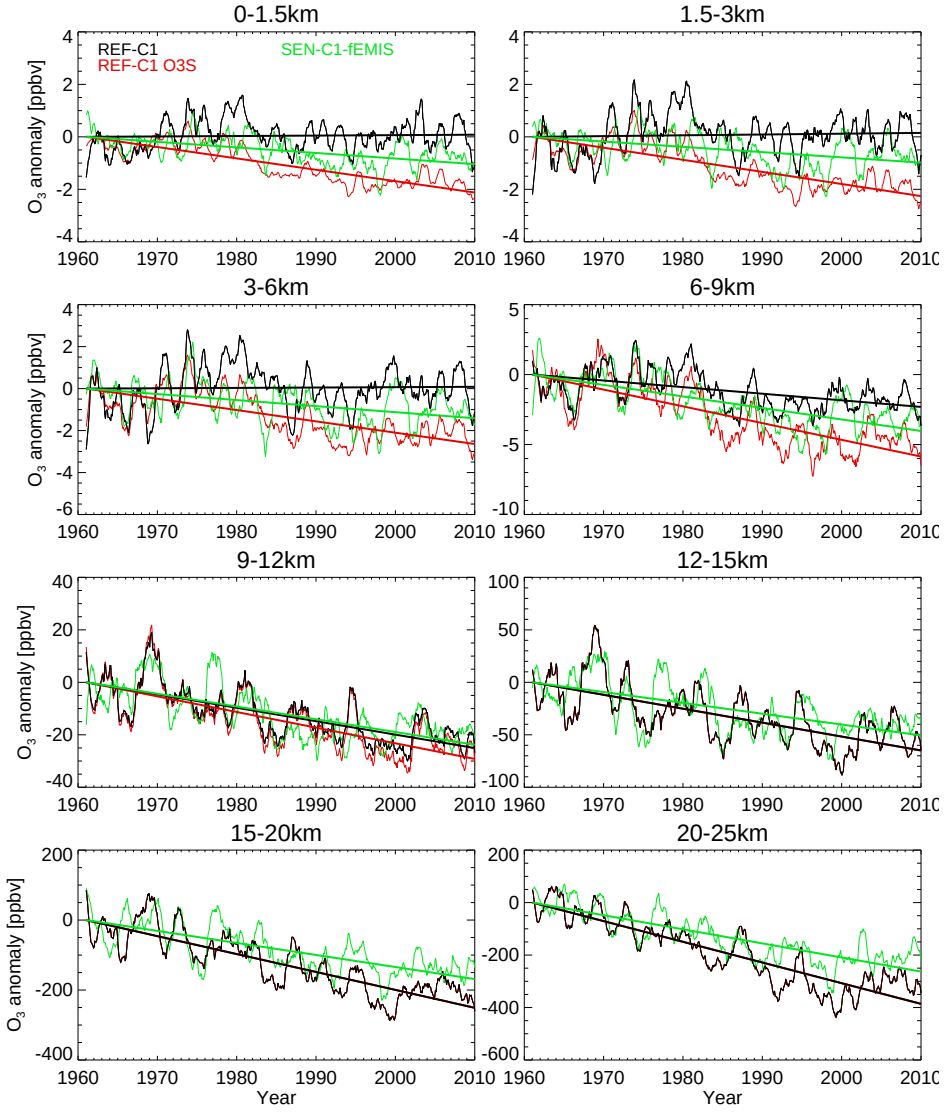

Figure 9. Modelled O_3 anomalies and linear trends at Lauder over 1960-2010 from REF-C1 (black) and SEN-C1-fEMIS (green), respectively. The anomaly and linear trend of stratospheric O_3 tracer (O_3S) are also depicted (red). Anomalies shown are smoothed with a 13-monthly filter for the purpose of display.

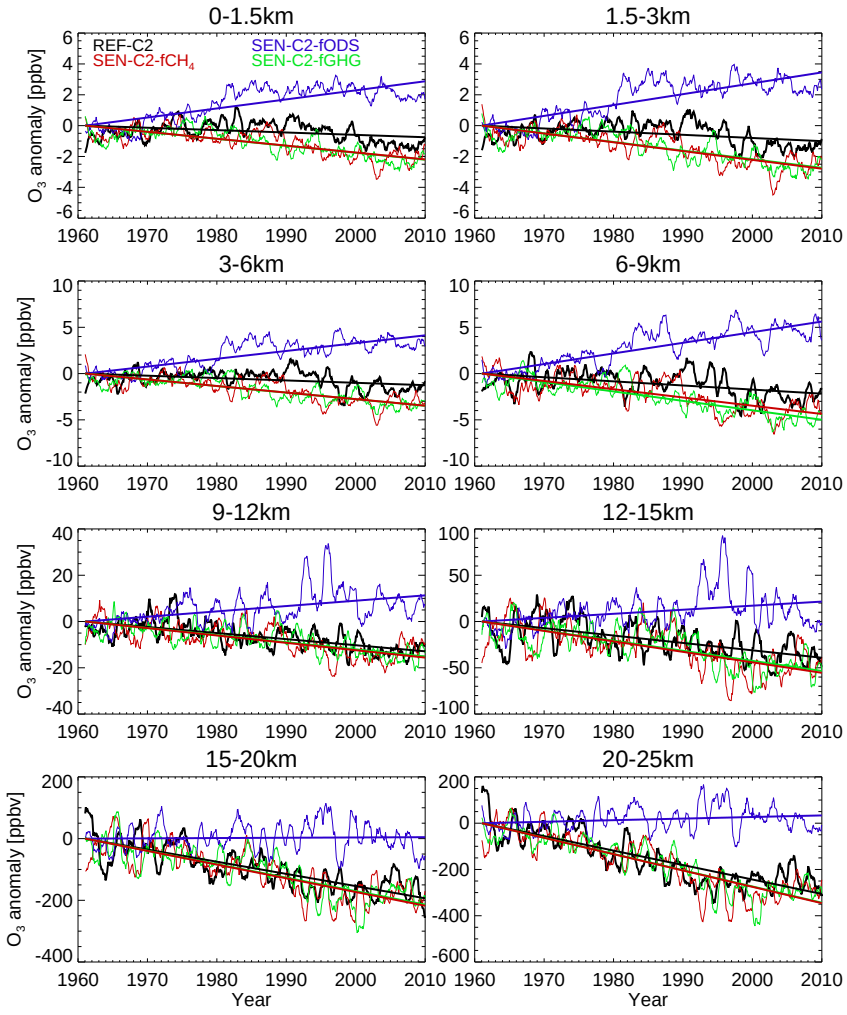

Figure 10. Modelled O_3 anomalies and linear trends at Lauder over 1960-2010, from REF-C2 (black), SEN-C2-fGHG (green), SEN-C2-fCH_4 (red), and SEN-C2-fODS (blue), respectively. Anomalies shown are smoothed with a 13-monthly filter for the purpose of display.